Acta Applicandae Mathematicae manuscript No.
(will be inserted by the editor)

Asymptotic analysis of boundary layers in a repulsive particle system

Cameron L. Hall · Thomas Hudson · Patrick van Meurs

Received: date / Accepted: date

Abstract This paper studies the boundary behaviour at mechanical equilibrium at the ends of a finite interval of a class of systems of interacting particles with monotone decreasing repulsive force. This setting covers, for instance, pile-ups of dislocations, dislocation dipoles and dislocation walls. The main challenge in characterising the boundary behaviour is to control the nonlocal nature of the pairwise particle interactions. Using matched asymptotic expansions for the particle positions and rigorous development of an appropriate energy via Γ–convergence, we obtain the equilibrium equation solved by the boundary layer correction, associate an energy with an appropriate scaling to this correction, and provide decay rates into the bulk.

Keywords Particle system · Boundary layer · Discrete-to-continuum asymptotics · Matched asymptotic expansions · Γ–convergence.

Mathematics Subject Classification (2000) 74Q05 · 74G10 · 41A60

1 Introduction

The analysis of particle systems is fundamental to a wide range of physical and mathematical problems. Many physical systems can be modelled by considering collections of interacting identical particles; examples include atoms in a fluid [25], charged particles in a

CLH acknowledges the support of the Mathematics Applications Consortium for Science and Industry, funded by the Science Foundation Ireland grant investigator award 12/IA/1683. The work of TH is funded by a public grant overseen by the French National Research Agency (ANR) as part of the "Investissements d'Avenir" program (reference: ANR-10-LABX-0098). The work of PvM is partially funded by NWO Complexity grant 645.000.012, and partially by the International Research Fellowship of the Japanese Society for the Promotion of Science, together with the JSPS KAKENHI grant 15F15019.

C. L. Hall
Department of Mathematics and Statistics, University of Limerick, Castletroy, Limerick, Ireland

T. Hudson
École des Ponts ParisTech, CERMICS, 6 et 8, Avenue Blaise Pascal, 77455 Champs-sur-Marne, France

P. van Meurs, Faculty of Mathematics and Physics, Kanazawa University, Kakuma, 920-1192, Kanazawa, Japan

supercapacitor [27], dislocations in a crystalline solid [22], Ginzburg–Landau vortices in a superconductor [2], spin states in an atomic lattice [33], collective behaviour of autonomous agents [1,10] and the generic problem of modelling a collection of hard spheres [29]. Additionally, the analysis of particle systems has applications to other areas of mathematics, most notably on the eigenvalues of random matrices [13,47]. A core challenge in studying particle systems is to predict the features of the thermodynamic equilibrium of a system where the number of particles is very large. At low temperatures, this is closely related to finding configurations with the lowest total potential energy, i.e. the *mechanical equilibria*.

Typically, low potential energy configurations in large particle systems exhibit *crystallisation* phenomena, i.e., particles arrange themselves into a periodic structure on the micro-scale with a slowly–varying density on the macro-scale [8,26,34,36]. However, this periodic structure on the micro-scale commonly breaks down close to any boundary of the domain; the density of particles near a boundary may vary on a microscopic or mesoscopic length-scale in ways that will not be captured by macro-scale descriptions of the particle density. All boundaries, including both free surfaces and rigid confining barriers, can lead to such anomalies. Boundary effects and other finite system size effects are a significant theme in current scientific research [5,18,24,34,37,43,46,48] since it is through boundary interactions that a large number of physical processes take place; important examples include contact [17], catalysis [42] and crystal growth [35].

We contribute to the current understanding of boundary effects by presenting an analysis of a one–dimensional system of particles (introduced in §1.1) interacting via a general repulsive pair potential and confined to a finite interval by rigid barriers. For this particle system, the Γ–convergence result in [16,31] implies that the equilibrium positions of the particles converge on the macro-scale in the many-particle limit to the constant particle density. As indicated before, such a convergence result is too coarse to determine boundary effects such as the force which the particles exert on the barriers.

Our main result (9) characterises the positions of the particles at equilibrium on the micro-scale close to the barriers in the many-particle limit. As a direct application of this result, we show in §1.3 how to compute the force which the particles exert on the barriers. Our analysis contributes to the literature on contact and fracture in crystalline solids [5,6, 23,37,40], dislocation pile-ups [15,19,20], and the collective behaviour of individual agents [1,10]. The novelty of our analysis is that we rely neither on a finite interaction range, nor on a specific expression for the interaction potential.

1.1 Setting

We suppose that $n+1$ identical particles are confined to lie in the interval $[0,n]$, and all pairs of particles mutually interact via a potential $V:\mathbb{R}\to[0,+\infty]$, which is a function of the inter-particle distance. Labelling the position of particle i as $\chi(i)$, the total potential energy of the system is thus

$$\sum_{k=1}^{n}\sum_{j=0}^{n-k} V\big(\chi(j+k)-\chi(j)\big).$$

Since we subsequently wish to consider the system with a large number of particles, it is convenient to introduce rescaled coordinates $x(i):=\chi(i)/n$, so that $x(i)\in[0,1]$ for all n. Applying this rescaling, we are led to consider the following equivalent scenario (see also

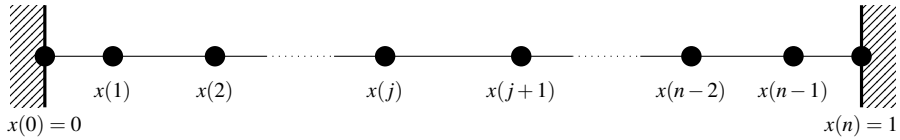

Fig. 1 The setting of the particle system in rescaled coordinates.

Figure 1), which is similar to that studied in [31]:

$$\mathscr{D}_n := \{x \in [0,1]^{n+1} \,|\, 0 =: x(0) \le x(1) \le \ldots \le x(n-1) \le x(n) := 1\},$$

$$E_n : \mathscr{D}_n \to [0,+\infty], \qquad E_n(x) := \frac{1}{n}\sum_{k=1}^{n}\sum_{j=0}^{n-k} V\big(n\big[x(j+k)-x(j)\big]\big).$$

Here, $\mathscr{D}_n$ represents the set of all possible valid positions, and $E_n(x)$ is the average energy per particle in the system due to the interactions with all the other particles in the configuration described by x. Our basic assumptions on the potential $V : \mathbb{R} \to [0,+\infty]$ are:

(Reg) $V : \mathbb{R} \setminus \{0\} \to (0,+\infty)$ is even and C^2;

(Sing) $V(x) \to V(0) = +\infty$ as $x \downarrow 0$ or $x \uparrow 0$;

(Cvx) for each $x \in (0,+\infty)$, there exists $\lambda(x) > 0$ such that V is $\lambda(x)$–convex on $(0,x)$, i.e.

$$\inf_{(0,x)} V'' \ge \lambda(x) > 0;$$

(Dec) $V(x), V'(x) \to 0$ as $|x| \to \infty$, and there exists $a > 1$ and constants c_δ such that for any $\delta > 0$,

$$V''(x) \le c_\delta |x|^{-a-2} \qquad \text{for any } x \in \mathbb{R} \setminus (-\delta,\delta).$$

Figure 2 shows a typical graph for such a potential V, and a prototypical example is $V(x) = |x|^{-a}$ with $a > 1$. We note the following immediate consequences of our basic assumptions:

- As V is non-negative, $E_n(x) \ge 0$.
- Together, **(Cvx)** and **(Dec)** demonstrate that V'' is integrable on $\mathbb{R} \setminus (-\delta,\delta)$, so by applying the Fundamental Theorem of Calculus on the interval $(x,+\infty)$, we find that there exist constants $c'_\delta, c''_\delta > 0$ and $a > 1$ such that

$$0 > V'(x) \ge -c'_\delta |x|^{-a-1} \quad \text{and} \quad 0 < V(x) \le c''_\delta |x|^{-a} \quad \text{for } x > \delta. \tag{1}$$

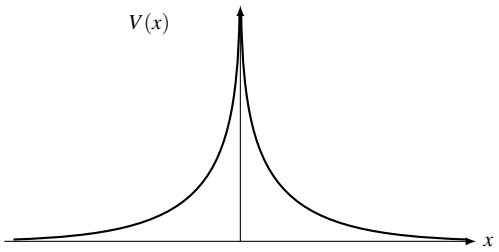

Fig. 2 Typical profile for the interaction potential V.

Since $V'(x) < 0$ for $x \in (0,\infty)$, the interactions are repulsive, and hence we must 'confine' the particles in order to ensure that they remain within a compact set: here, our choice is to enforce confinement by fixing the outermost particles.

– As observed in [16,31], **(Cvx)** implies that E_n is strictly convex on $\mathscr{D}_n$. Moreover, **(Sing)** makes the energy infinite on the set

$$\partial\mathscr{D}_n := \big\{x \in \mathscr{D}_n \,\big|\, x(i-1) = x(i) \text{ for some } i \in \{1,\dots,n\}\big\}.$$

Therefore, E_n has a unique stable equilibrium, which is contained in $\mathscr{D}_n \setminus \partial\mathscr{D}_n$. Since E_n is differentiable on this set, the equilibrium satisfies the following force balance:

$$\frac{\partial E_n(x)}{\partial x(i)} = -\sum_{\substack{k=0\\k\neq i}}^{n} V'\big(n[x(k)-x(i)]\big) = 0, \qquad i = 1,\dots,n-1. \tag{2}$$

1.2 Main results

In [16,31], it was shown that E_n Γ–converges, and that the limit energy has a unique minimiser corresponding to a uniform density of particles. Since the topology used to obtain these previous Γ–convergence results (i.e. the narrow or weak topology of measures) cannot detect 'microscopic' variations in particle density, we strengthen these convergence results by obtaining a finer characterisation of the minimiser of E_n. In particular, we seek to describe the *boundary layers* which appear at both ends of the bounded interval; see Figure 3 for a numerical illustration. To do so, we use two different approaches: formal asymptotic analysis [21] and Γ–development of the energy E_n [4,7,12]. Our formal analysis gives us a detailed description of the equilibrium particle positions in the boundary layers when n is large enough, while the Γ–development establishes a precise notion of convergence for the particle positions and boundary-layer energy as $n \to \infty$.

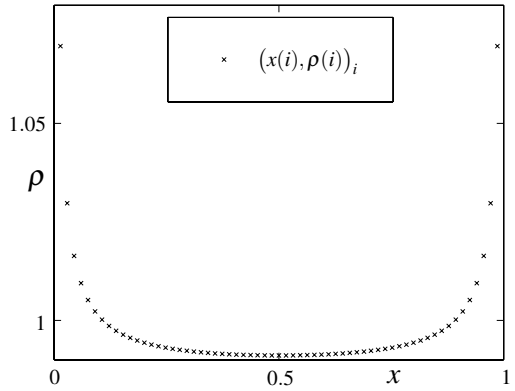

Fig. 3 Equilibrium configuration of $n+1 = 65$ particles $x(i)$ (i.e. the solution to (2)) for the potential $V(x) = x^{-2}$. The horizontal axis shows the domain $[0,1]$. The vertical axis measures the 'discrete density' defined by $\rho(i) := 2/(n[x(i+1)-x(i-1)])$.

In §2, formal asymptotic analysis is used both to obtain the equations of equilibrium in the bulk, and to show that the correct scaling for the boundary layer is in terms of the particle

positions $\chi(i) = nx(i)$, with no intermediate regime between the bulk and discrete scaling. To carry out this analysis, we require a slightly stronger condition on the differentiability of V, and so in this section, as well as the basic assumptions detailed in §1.1, we require the additional regularity assumption

(Reg+) $V \in C^3(0,\infty)$, with $|V'''(x)| \lesssim |x|^{-a-3}$ for $|x| > 1$.

In §2.4, this permits us to obtain the result that the particle positions $\chi(i)$ in the boundary layer approximate the solution of the following infinite system of equations as $n \to \infty$:

$$\begin{cases} 0 = \displaystyle\sum_{\substack{k=0 \\ k\neq i}}^{\infty} V'\big[\chi(i) - \chi(k)\big], & i = 1,2,3,\ldots, \\ \chi(i) - \chi(i-1) = 1 + o(1), & \text{as } i \to \infty. \end{cases} \tag{3}$$

In §3, with technical details given in Appendix A, we again use formal methods to obtain further terms in an asymptotic expansion of both the boundary layer and the bulk behaviour in the particular case $V(x) = |x|^{-a}$, which is the prototypical potential satisfying the assumptions detailed in §1.1. Using the method of matched asymptotic expansions, we fully characterise particle locations in both the bulk and the boundary layer up to errors that are asymptotically smaller than $n^{-(a-1)}$ as $n \to \infty$. To the best of our knowledge, this characterisation of higher order terms in the asymptotic expansion for particle systems with nonlocal interactions is new.

Additionally, this analysis allows us to characterise the behaviour of $\chi(i)$, the solution to (3), as $i \to \infty$ by a more detailed description of the $o(1)$ term. When $V(x) = |x|^{-a}$, we find that

$$\chi(i) - \chi(i-1) = 1 - \frac{i^{-(a-1)}}{\zeta(a)(a^3-a)} + o[i^{-(a-1)}], \quad \text{as } i \to \infty, \tag{4}$$

where $\zeta(s)$ is the Riemann zeta function. In fact, this decay behaviour of χ remains valid for more general potential V satisfying **(Reg)**, **(Sing)** and **(Cvx)** whenever the tails of $V^{(k)}$ are asymptotically equivalent to $d^k/dx^k\,(x^{-a})$ up to sufficiently large k (see (30) for details). In that case, the constant $[\zeta(a)(a^3-a)]^{-1}$ takes the more general form $[(a-1)\sum_{j=1}^{\infty} V''(j)j^2]^{-1}$.

The formal asymptotic analysis leaves us with two questions associated with general case treated in §2: what is the proper space in which to seek solutions χ to (3), and in what sense do the solutions of (2) converge to solutions of (3) as $n \to \infty$? In §4, we address these question by proving a Γ–convergence result. This proof rests upon a different strengthening of our basic assumptions, requiring the stronger decay hypothesis

(Dec+) $V(x), V'(x) \to 0$ as $|x| \to \infty$, and there exists $a > \frac{3}{2}$ and constants c_δ such that for any $\delta > 0$,

$$V''(x) \leq c_\delta |x|^{-a-2} \qquad \text{for any } x \in \mathbb{R} \setminus (-\delta, \delta).$$

Under both our basic assumptions and this extra assumption, we prove Theorem 43, demonstrating Γ–convergence of the 'renormalised' energy

$$E_n^1(x) := nE_n(x) - \sum_{k=1}^{n} (n-k+1)V(k). \tag{5}$$

This energy is renormalised in the sense that the subtracted term need not be bounded as $n \to \infty$. To treat E_n^1 more easily and obtain a useful compactness result, we introduce a convenient change of variable given by

$$\varepsilon(i) := n\big[x(i) - x(i-1)\big] - 1 \qquad \text{for } i = 1, \dots, n. \tag{6}$$

The choice to use ε here as notation is due to the analogy with the infinitesimal strain used in continuum mechanics, since ε measures how far the particles deviate from being equispaced.

The system §2 obtained by formal asymptotic analysis suggests that $\varepsilon(i) = \chi(i) - \chi(i-1) - 1 \to 0$ as $n \to \infty$ and $1 \ll i \ll n$. In fact, the compactness statement of Theorem 43 states that boundedness of $E_n^1(\varepsilon)$ implies boundedness of ε in $\ell^2(\mathbb{N})$, which will subsequently allow us to give a precise meaning to this statement. Taking the Γ–limit as $n \to \infty$, E_n^1 splits into two independent, similar terms: E_∞^l for the energy of the boundary layer at the left (l) barrier, and E_∞^r for the energy of the boundary layer at the right (r) barrier. More specifically,

$$\begin{aligned} E_\infty^l &: \big\{\varepsilon \in \ell^2(\mathbb{N}) \,\big|\, \varepsilon(i) \geq -1 \ \forall\, i \geq 1\big\} \to \overline{\mathbb{R}}, \\ E_\infty^l(\varepsilon) &:= \sum_{k=1}^{\infty} \sum_{j=0}^{\infty} \phi_k\Bigg(\sum_{l=j+1}^{k+j} \varepsilon(l) \Bigg) + (\sigma^\infty, \varepsilon)_{\ell^2(\mathbb{N})}, \end{aligned} \tag{7}$$

where $\sigma^\infty \in \ell^2(\mathbb{N})$ and $\phi_k : (-k, \infty) \to [0, \infty)$ are given by

$$\begin{aligned} \sigma^\infty(i) &:= \sum_{k=i+1}^{\infty} (k-i)\big|V'(k)\big|, \quad \text{and} \\ \phi_k(y) &:= V(k+y) - V(k) - V'(k)y. \end{aligned} \tag{8}$$

We note that ϕ_k is the residual of the first-order Taylor approximation of V at k, which is non-negative because of **(Cvx)**. The sequence σ^∞ accounts for the contribution of the first-order Taylor approximation of V to the energy E_∞^l, and may be thought of as a stress induced on the boundary layer by the presence of the bulk.

In Lemma 45 we prove existence and uniqueness of minimisers for E_∞^l in $\ell^2(\mathbb{N})$. Moreover, we show that the related infinite set of Euler-Lagrange equations is equivalent to solving

$$\begin{cases} 0 = \displaystyle\sum_{\substack{k=0 \\ k \neq i}}^{\infty} V'\big[\chi(i) - \chi(k)\big], \quad i = 1, 2, 3, \dots, \\ \big(\chi(i) - \chi(i-1) - 1\big)_{i \in \mathbb{N}} \in \big\{\varepsilon \in \ell^2(\mathbb{N}) \,\big|\, \varepsilon(i) \geq -1 \ \forall\, i \geq 1\big\}. \end{cases} \tag{9}$$

This therefore provides us with a precise characterisation of solutions to (3).

In §5, we conclude by describing a numerical method for solving (9). The numerical scheme approximates (9) by assuming that $\chi(i) = \chi(i-1) + 1$ for all i larger than a fixed index. We compare its solution to the minimiser x^n of (2) for various numbers of n particles and for two physically relevant choices for V: the case of dislocation dipoles ([20], $V(x) = x^{-2}$) and dislocation walls ([15], V has a logarithmic singularity at 0 and tails which vanish exponentially fast; see (53)). We observe that the convergence rate of $nx^n(i)$ to $\chi(i)$ as $n \to \infty$ is close to $O(n^{-1})$, and independent of i. Furthermore, we find that the boundary layer profiles are qualitatively *different* for the two choices of V, even though they satisfy all imposed conditions, and hence resemble the graph in Figure 2.

1.3 Discussion and conclusion

The main fruits of our analysis are (4) and (9). Equation (9) is significant because it provides us with a characterisation of the boundary layer behaviour in terms of an infinite system of discrete equations. In particular, the boundary condition in (9) gives a precise meaning to the idea that the particles are 'equispaced' in the bulk; by showing that (9) has a unique solution for χ where $\chi(i)-\chi(i-1)-1 \in \ell^2(\mathbb{N})$, we place asymptotic limits on the extent to which the energy-minimising particle configuration can deviate from equal spacing. Moreover, the fact that we are able to obtain (9) from an asymptotic development of the ground state energy represents a significant theoretical advance for the treatment of discrete-scale boundary layers using Γ–convergence. In previous work, such as [5,15,23,37], either only finite interaction ranges or continuum-scale boundary layers were considered. Figure 4 illustrates the discrete-scale boundary layer in the case where $V(x) = |x|^{-2}$, showing that the solution to (9) provides a good asymptotic approximation to the solution of the full problem.

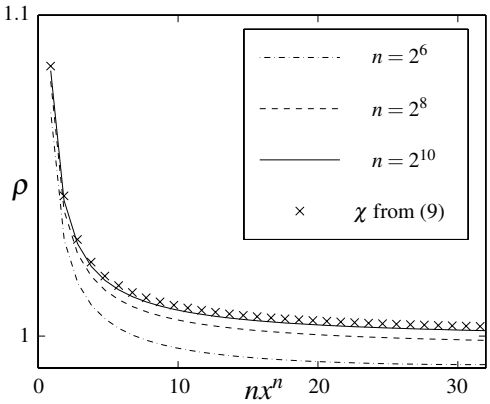

Fig. 4 The three line graphs depict the 'discrete' density of the minimiser x^n of E_n for $n = 2^6, 2^8, 2^{10}$ and $V(x) = x^{-2}$, in the rescaled coordinates $\chi^n := nx^n$. The graph of $n = 2^6$ corresponds to Figure 3. The three line graphs indicate the convergence to the boundary layer profile computed from χ ($\times$), which is here the solution to (9). See Figure 9 for the definition of the 'discrete' density.

Equation (4) is significant because it gives explicit form to the tail behaviour of the boundary layer solution in the case of a homogeneous potential (that is, a potential V is homogeneous is there exists a $b \in \mathbb{R}$ such that V is b-homogeneous, i.e., $V(\alpha x) = \alpha^b V(x)$ for all $\alpha > 0$ and all $x > 0$). While (4) is only directly relevant in the case where $V(x) = |x|^{-a}$, it hints at why the analysis in §4 relies on the assumption that $a > \frac{3}{2}$ in **(Dec+)**. In the case where $1 < a \leq \frac{3}{2}$, (4) indicates that the associated $\varepsilon(i) := \chi(i) - \chi(i-1) - 1$ is not in $\ell^2(\mathbb{N})$, and hence a new scaling and finer analysis will be necessary to recover the correct energetic description using Γ–convergence; in fact, we show in §4.5 that taking the limit functional E^l_∞ with a potential for which $a < 3/2$ leads to an ill–posed variational problem. The derivation of (4) in §3 does however suggest some of the tools necessary to extend our analysis: in the case where $1 < a \leq \frac{3}{2}$ it appears that the contributions from singular integral terms are important. We might therefore expect that §4 can be extended to $a \leq \frac{3}{2}$ by seeking a bulk correction to the total energy associated with nonlocal interactions between particles.

We now discuss our assumptions and findings as well as their implications in more detail.

Choice of scaling. The particular choice of scaling made here, i.e., taking the length of the domain to depend linearly on the number of particles, is the usual choice made when considering the thermodynamic limit of a system with a fixed number of particles per unit volume [3,6]. In other physical situations, other scalings may be more appropriate, and may lead to different energetic descriptions; see for example [15,16].

Matched asymptotic analysis versus Γ–convergence. In keeping with other studies, we observe that the advantage of matched asymptotic analysis is the ease and flexibility of the arguments with which we obtain equation (3): it requires a less detailed analysis than the Γ–convergence result, relying upon on a well–chosen ansatz for the asymptotic development of the solution. On the other hand, the main advantage of the Γ–convergence statement is that it implies well–posedness of (9), and with it the development of the ground state energy for E_n. However, the analysis relies on the minimiser being close to the equispaced configuration, which makes it harder to apply, e.g., when a constant external stress is applied to the particles.

In the broader mathematical context of modelling particle systems, our approach suggests that combining formal asymptotics with Γ–convergence techniques can be fruitful for understanding boundary effects in particle systems with more general long–range interactions.

Asymptotic equilibrium problem. The infinite sum in (3) does *not* simply correspond to replacing n by ∞ in the force balance in (2). Instead, (3) has two elements; the first equation in (3) is obtained by rescaling (2) for the boundary layer case where $i = O(1)$ as $n \to \infty$, while the second equation in (3) is associated with a matching condition between the boundary layer solution and the bulk solution.

Comparison with [20]. In [20], formal asymptotic methods were used to analyse the problem of a pile-up of repulsive particles against a single fixed obstacle, driven by a constant external force. In the present work, we consider a similar problem where the particles are trapped in between two fixed obstacles. However, our formal asymptotic analysis provides two significant extensions to the results in [20]. First, in §2 we dispense with the assumption used in [20] that V is $-a$-homogeneous, and obtain a leading-order asymptotic solution for a general V. This is novel in the formal asymptotics literature on discrete problems. Second, in §3 we reintroduce the assumption that V is $-a$-homogeneous, and extend the asymptotic analysis in [20] to include many higher-order corrections. Using this method, we are able to obtain a more precise description of the matching condition between the bulk and the boundary layer.

Comparison with [15]. The setting in [15] corresponds to changing the choice of scaling for the domain from $[0,n]$ made here to $[0,c_n]$ for some $1 \ll c_n \ll n$. The observed boundary layer consists of $O(n/c_n)$ particles, and is therefore expected to be described by a *continuous* profile in the many–particle limit. In this paper, $c_n = n$, and while we also find that the boundary layer consists of $O(n/c_n) = O(1)$ particles, this means instead that the boundary layer profile remains *discrete* in the many–particle limit. We see the effect of these different scaling regimes reflected in the assumptions on V; while the analysis in [15] relies on less regularity and a weaker notion than convexity of V, we weaken the assumption of finite first moments on the tails of V (which is slightly stronger than $a \geq 2$).

Other forms of confinement. A physically–interesting extension of our scenario is to consider the system subject to a constant external stress term which pushes the particles to

one of the two barriers, in place of one or both of the rigid boundary constraints that we consider. Such a constraint results in a free–boundary problem: examples of such scenarios are examined in, e.g., [16,20,31]. While we expect our asymptotic analysis to apply with some modifications along the lines of [19,20], our Γ–convergence analysis would require us to find an appropriate variable to describe the free boundary, and then to obtain *a priori* estimates in this variable, similar to those given in §4.2. This appears to be a significant challenge, but with appropriate intuition developed via formal asymptotics, this may be possible in the future.

Force on the boundary. As mentioned before, one important boundary effect is the force that the particles at equilibrium exert on the barriers. From (2) we obtain that this force is given by

$$F_n(x) := -\sum_{i=1}^{n} V'(nx(i)), \tag{10}$$

where $x \in \mathscr{D}_n$ minimises E_n. Computing $F_n(x)$ is relevant, for instance, in contact problems [17] or dislocation pile-ups [22].

The result in [16,31] that the minimiser of E_n converge on the macro-scale to the constant density is too coarse to give a direct prediction for $F_n(x)$. A natural, indirect manner to approximate $F_n(x)$ from the constant density profile is to reconstruct the particle positions as being equispaced, i.e., $(\frac{i}{n})_{i=0}^n \in \mathscr{D}_n$. Due to **(Dec)**, we obtain

$$F_n\big((\tfrac{i}{n})_{i=0}^n\big) = -\sum_{i=1}^{n} V'(i) \xrightarrow{n\to\infty} -\sum_{i=1}^{\infty} V'(i) =: \tilde{F}, \tag{11}$$

where $\tilde{F} \in \mathbb{R}$ approximates the force on the boundary induced by the equispaced configuration for large n.

The solution χ to the boundary layer problem (9) gives an improved approximation of the particle positions at the barrier. It predicts the following force on the boundary

$$F(\chi) = -\sum_{k=1}^{\infty} V'(\chi(i)), \tag{12}$$

which can be computed independent of n. From the numerical computations summarised in Table 2 we observe that $F(\chi)$ is a good approximation of $F_n(x)$. Moreover, $F(\chi) > \tilde{F}$, which shows that the naive prediction $\tilde{F}$ *undershoots* the actual force on the barrier. We believe that this result is relevant beyond contact problems and dislocation pile-ups, especially if it can be extended to higher-dimensional scenarios and attractive–repulsive interaction potentials.

Higher–dimensional problems. Many of the models described in the introduction have a greater physical relevance in higher dimensions. However, in higher dimensions the characterisation of minimisers is significantly more challenging because of the greater geometric freedom of the particle positions and the loss of a natural ordering for the particles. Nevertheless, as explained in the introduction, there is evidence that minimisers exhibit crystallisation in many situations, in which case our results can still be used to approximate boundary effects.

Consider, for instance, the question of finding the force on the boundary induced by n repulsive particles confined to lie in a polygonal set. Assuming that, for large n, the particles are close to a crystal structure near a flat part of the boundary, the minimiser is a configuration which is approximately periodic in the direction tangential to the boundary. Viewing the lines of particles tangential to the boundary as "walls" of particles, the problem is approximated in the normal direction to the boundary by a one–dimensional particle system of

particle walls interacting by an effective potential. For this one–dimensional particle system, the force on the boundary exerted by the particles is given by (12). This value could provide a reasonable approximation for the actual force on the boundary.

Attractive–repulsive interactions. As discussed in the introduction, many particle systems relevant for applications exhibit interactions which combine both attractive and repulsive behaviour. Examples include the atomistic models of crystalline materials [5, 14, 23, 37, 41], swarming models in biology [1], and crowd dynamics models [10]. To the best of our knowledge, there are no results yet concerning the analysis of boundary layers in such systems without assuming that interactions have finite range. Moreover, in higher dimensions the additional challenge is to deal with very large numbers of local minima [44]. Nevertheless, our approach here suggests a possible methodology: by using formal asymptotic methods to first obtain approximations of equilibrium states, the properties of minimisers can be used to gain intuition concerning the correct functional analytic framework in which to establish a Γ–convergence result. We expect the key challenge to be to obtain a suitable compactness result which appropriately captures free boundary behaviour.

Dynamics of particles. Our results focus on properties of the equilibrium configuration of the system, since our assumption of repulsive interactions guarantees a unique stable equilibrium. A natural extension for further study is to understand an appropriate evolution of the particles close to the barriers. While gradient–flow dynamics have been obtained in [30] for the density of particles on the macro-scale, a correction for the evolution of the particles close to the barrier remains elusive. Such a correction is needed, for instance, for understanding how lattice waves scatter off of the ends of the domain, since this has relevance for *in situ* observation of crystal plasticity [38]. Our result on the particle positions at equilibrium (9) provides a possible starting point for a future study in this direction.

The remainder of the paper is organised as follows. In §2 we perform the asymptotic analysis to derive the boundary layer equation (3) from the force balance (2) in the general case. In §3 we summarise how to obtain higher–order corrections in the specific case where $V(x) = |x|^{-a}$; the computations are left to Appendix A. In §4 we establish Γ–convergence of the energy difference E_n^1, and show how it connects the force balance (2) to the description of the boundary layer in (9). The details of the proofs are documented in Appendix B. Finally, in §5, we give numerical examples validating our asymptotic development for two physically relevant choices of V.

2 Formal asymptotic analysis – Leading order analysis for $a > 1$

2.1 Notation and preliminaries

We begin by using classical formal asymptotic methods analogous to those in [20] to obtain the leading-order asymptotic solution to the system of algebraic equations given in (2). The novelty of our approach here is that it relies only upon the basic assumptions on V detailed in §1.1 and **(Reg+)**, and not on an explicit choice of potential as in [20].

To clarify the notation which is used throughout this section, §3 and Appendix A, we include Table 1 for the reader's convenience: the notation is equivalent to that used in [21].

Supposing that $x(i;n)$ solves the system of equilibrium equations (2) for a given n, and following [20], we propose the following ansatz for an approximate solution in the bulk:

$$x(i;n) = \xi(in^{-1};n), \tag{13}$$

Table 1 Asymptotic notation. All definitions are interpreted in the limit $n \to \infty$.

Notation	Definition
$f(n) = O(g(n))$	$\exists C > 0$ such that $\lvert f(n)\rvert \le C\lvert g(n)\rvert$
$f(n) = \operatorname{ord}(g(n))$	$\exists C > 0$ such that $\limsup \lvert f(n)\rvert/\lvert g(n)\rvert = C$
$f(n) = o(g(n))$	$\lvert f(n)\rvert/\lvert g(n)\rvert \to 0$
$f(n) \ll g(n)$	$\lvert f(n)\rvert/\lvert g(n)\rvert \to 0$
$f(n) \sim \sum_{i=1}^{\infty} g_i(n)$	$\forall k \in \mathbb{N}$, $f(n) - \sum_{i=1}^{k} g_i(n) = O(g_{k+1}(n))$
$f(n) \sim \sum_{i=1}^{N} g_i(n)$	$\forall k \le N-1$, $f(n) - \sum_{i=1}^{k} g_i(n) = O(g_{k+1}(n))$, $f(n) - \sum_{i=1}^{N} g_i(n) = o(g_N(n))$

where $\xi(s;n)$ is expanded as an asymptotic power series

$$\xi(s;n) \sim \xi_0(s) + n^{-b_1}\xi_1(s) + n^{-b_2}\xi_2(s) + \dots, \tag{14}$$

with b_i strictly increasing. For convenience, we simply write $x(i)$ and $\xi(s)$ whenever possible, omitting their dependence upon n.

Following convention, we treat ξ as though it were a function, even though the series definition of ξ in (14) is an asymptotic series, and therefore may not converge for any fixed s and n. Strictly speaking, equations involving ξ should be interpreted as being true for fixed s in the asymptotic limit as $n \to \infty$ where any instance of $\xi(s)$ is read as

$$\xi(s) = \sum_{k=0}^{Q} n^{-b_k}\xi_k(s) + O\big(n^{-b_{Q+1}}\big),$$

for any choice of integer Q.

As we discuss in §2.3 and §2.4, we encounter boundary layers when s is sufficiently close to 0 or 1. As a result of these, we find that we will not be able to use the ansatz in (13) and (14) to describe particle positions when i is too close to 0 or n; instead, different ansatzes will be needed. In our higher-order analysis in §3, we are careful to take account of the effects of the boundary layer from the beginning of our analysis, but in this section we begin by assuming that (13) and (14) can be applied everywhere. While this is not strictly true (and would lead to contradictions if the analysis were extended to higher orders), identical results could be obtained by following the methods described in §A.1, where we use separate ansatzes for the bulk and the boundary layer from the outset.

Due to the boundary conditions $x(0) = 0$ and $x(n) = 1$, we assume that $\xi(0) = 0$ and $\xi(1) = 1$. In practice, these boundary conditions will only be satisfied to leading order, so that we apply them as

$$\xi_0(0) = 0 \qquad \text{and} \qquad \xi_0(1) = 1. \tag{15}$$

Additionally, we assume that $\xi(s)$ has the following smoothness and monotonicity properties:

(ξ-Smooth) $\xi \in C^4([0,1])$;
(ξ-Mon) ξ' is strictly positive, i.e. there exists $M > 0$ such that $\xi'(s) \ge M$ for all $s \in [0,1]$.

The monotonicity assumption **(ξ-Mon)** implies that

$$\chi(i+1) - \chi(i) = n[x(i+1) - x(i)] = n\int_{i/n}^{(i+1)/n} \xi'(s)\,\mathrm{d}s \ge M.$$

That is, we assume that at equilibrium no two particles are closer than M/n, uniformly in n, and thus the particle density is uniformly bounded. This is a natural assumption as long

as the long-range interactions between particles are not strong enough to make very high densities of particles favourable as $n \to \infty$.

Since ξ is a continuous object, it is natural to cast the discrete force balance in (2) in a continuous form as well. By separating the interactions with the neighbours on the left from those on the right, we rewrite (2) as

$$F(s) = 0, \quad \text{for all } s = \frac{1}{n}, \dots, \frac{n-1}{n}, \tag{16}$$

$$F(s) := \sum_{k=1}^{\lfloor n-sn \rfloor} V'\big(n\big[\xi(s+kn^{-1}) - \xi(s)\big]\big) - \sum_{k=1}^{\lfloor sn \rfloor} V'\big(n\big[\xi(s) - \xi(s-kn^{-1})\big]\big). \tag{17}$$

In Section 2.2, we manipulate this definition of $F(s)$ in order to obtain the leading-order dependence of F on ξ as $n \to \infty$. From this, we can obtain an equation for $\xi_0(s)$ and hence an asymptotic expression for the equilibrium particle locations in the bulk.

2.2 Asymptotic analysis using the bulk ansatz

In the analysis below, we show that $F(s)$ is given asymptotically by

$$F(s) = n^{-1}\xi''(s) \sum_{k=1}^{\infty} \big(V''\big[\xi'(s)k\big]k^2\big) + o(n^{-1}), \tag{18}$$

so long as $s \gg n^{-\frac{1}{a}}$ and $1 - s \gg n^{-\frac{1}{a}}$. To this end, we introduce an arbitrary integer H where $n^{\frac{1}{a}} \ll H \ll n$, and split the sums in (17) as follows:

$$\begin{aligned} F(s) = &\underbrace{\sum_{k=1}^{H} \Big[V'\big(n\big[\xi(s+kn^{-1}) - \xi(s)\big]\big) - V'\big(n\big[\xi(s) - \xi(s-kn^{-1})\big]\big)\Big]}_{=:S_1} \\ &+ \underbrace{\sum_{k=1}^{\lfloor n-sn \rfloor - H} V'\big(n\big[\xi(s+Hn^{-1}+kn^{-1}) - \xi(s)\big]\big)}_{=:S_2} \\ &- \underbrace{\sum_{k=1}^{\lfloor sn \rfloor - H} V'\big(n\big[\xi(s) - \xi(s-Hn^{-1}-kn^{-1})\big]\big)}_{=:S_3}. \end{aligned} \tag{19}$$

We observe from **(ξ-Mon)** that the argument of V' in the sums S_2 and S_3 is bounded from below by $M(H+k)$. Then, using the fact that **(Dec)** and **(Cvx)** imply (1), the summands in S_2 and S_3 are bounded in absolute value by $c'_\delta M^{-a-1}(H+k)^{-a-1}$. Therefore,

$$|S_2| + |S_3| \le 2\sum_{k=1}^{\infty} c'_\delta M^{-a-1}(H+k)^{-a-1} \lesssim H^{-a} = o(n^{-1}).$$

To expand S_1 in terms of n, we repeatedly employ Taylor's theorem. More precisely, using the regularity of V and ξ as given by **(Reg+)** and **(ξ-Smooth)**, we write

$$\begin{aligned} V'(x+\delta) &= V'(x) + V''(x)\delta + \tfrac{1}{2}V'''(x+\theta_\delta\delta)\delta^2, \\ \xi(s+\delta) &= \xi(s) + \xi'(s)\delta + \tfrac{1}{2}\xi''(s)\delta^2 + \tfrac{1}{6}\xi'''(s+\rho_\delta\delta)\delta^3, \end{aligned}$$

for some $\theta_\delta, \rho_\delta \in [0,1]$. Moreover, **(Reg+)** implies that

$$V'''(x+\theta_\delta\delta)\delta^2 = \delta^2 \cdot O(x^{-a-3}) \quad \text{as } x \to \infty,$$

as long as $\delta \ll x$.

We now apply the Taylor expansion of ξ to the arguments of V' in S_1. By the uniform continuity of ξ''', we obtain

$$\begin{aligned} n\big[\xi(s \pm kn^{-1}) - \xi(s)\big] &= n\big[\pm\xi'(s)kn^{-1} + \tfrac{1}{2}\xi''(s)k^2n^{-2} + O\big(k^3n^{-3}\big)\big], \\ &= \pm k\xi'(s) + k\Big[\tfrac{1}{2}\xi''(s)kn^{-1} + O\big(k^2n^{-2}\big)\Big] \end{aligned}$$

as long as $k \ll n$. Moreover, since $H \ll n$, we see that $kn^{-1} \le Hn^{-1} \ll 1$ throughout the sum given in S_1. Applying the Taylor expansion of V and using the oddness of V' and evenness of V'', we find that

$$\begin{aligned} S_1 = \sum_{k=1}^{H} \Big[& V''\big[k\xi'(s)\big]\xi''(s)k^2n^{-1} + V''\big[k\xi'(s)\big]k \cdot O(k^2n^{-2}) \\ & + V'''\big[k\xi'(s) + \theta_k k \cdot O(kn^{-1})\big]k^2 \cdot O\big(k^2n^{-2}\big) \\ & + V'''\big[-k\xi'(s) - \theta_{-k}k \cdot O(kn^{-1})\big]k^2 \cdot O\big(k^2n^{-2}\big)\Big]. \end{aligned} \tag{20}$$

We now show that the sum of the last three of the four terms in the summand of (20) is $o(n^{-1})$. To treat the second term, we note that $V''[\xi'(s)k] = O(k^{-a-2})$ as $kn^{-1} \to 0$ and $k \to \infty$, and hence

$$V''\big[\xi'(s)k\big]k \cdot O(k^2n^{-2}) = O(k^{1-a}n^{-2}).$$

We sum to find that

$$\sum_{k=1}^{H} V''\big[\xi'(s)k\big]k \cdot O(k^2n^{-2}) = \begin{cases} O\big(H^{2-a}n^{-2}\big) & a \in (1,2), \\ O\big(\log(H)n^{-2}\big) & a = 2, \\ O(n^{-2}) & a > 2. \end{cases} \tag{21}$$

In all three cases, the fact that $H \gg n^{\frac{1}{a}}$ implies that the sum in (21) is $o(n^{-1})$.

To bound the third and fourth term in the summand of (20), we first observe that

$$V'''\big[\pm k\xi'(s) \pm \theta_{\pm k}k \cdot O(kn^{-1})\big] = O(k^{-3-a})$$

as long as $kn^{-1} \ll 1$. Hence

$$V'''\big[\pm k\xi'(s) \pm \theta_{\pm k}k \cdot O(kn^{-1})\big]k^2 \cdot O(k^2n^{-2}) = O(k^{1-a}n^{-2}),$$

and an analogous argument to that used to obtain (21) implies

$$S_1 = n^{-1}\sum_{k=1}^{H}\Big[\xi''(s)V''\big[\xi'(s)k\big]k^2\Big] + o(n^{-1}).$$

Finally, to obtain (18), we use $V''\big[\xi'(s)k\big]k^2 = O(k^{-a})$ to deduce that

$$\sum_{k=H+1}^{\infty}\Big[\xi''(s)V''\big[\xi'(s)k\big]k^2\Big] = O(H^{1-a}).$$

Since $H \gg 1$, adding this term does not change (19) at leading order, and we conclude that (18) holds.

Next, we investigate the implications of (16) and (18) for our ansatz in (13). Since ξ' is assumed to be bounded, the property **(Cvx)** implies that the sum in (18) is bounded from below by a positive constant. We conclude that the leading order density satisfies $\xi_0''(s) = 0$ whenever s is in an appropriate range. As argued in [20], we apply the boundary conditions $\xi_0(0) = 0$ and $\xi_0(1) = 1$ to $\xi_0''(s) = 0$, because possible boundary layers can only affect higher order corrections to the particle positions in the bulk. Consequently,

$$\xi_0(s) = s.$$

2.3 Investigating a continuum rescaling for the boundary layer

Our derivation of (18) relies on the assumption that $H \ll sn \ll n - H$ for some H with $n^{\frac{1}{a}} \ll H$. Hence, we cannot be confident that $\xi(s) \sim s$ is a valid leading-order approximation of the particle positions when $s = O(n^{-\frac{a-1}{a}})$ or when $s = 1 - O(n^{-\frac{a-1}{a}})$. To investigate these regimes fully, a new ansatz is therefore required.

When i or $n - i$ are sufficiently small, we may expect to see boundary layers where the original bulk scalings no longer apply; for an example of boundary layer analysis for a similar system, see [20]. The fact that the bulk ansatz is applicable when $i \gg n^{\frac{1}{a}}$ and $n - i \gg n^{\frac{1}{a}}$ indicates that the boundary layer width can be no greater than $\mathrm{ord}(n^{\frac{1}{a}})$.

To find the boundary layer rescaling, we follow a similar procedure to that used for classical problems from differential equations. We propose a new scaling of the variables, and analyse it to determine whether it yields a 'distinguished limit' where there is a new dominant balance between terms. Because of the symmetric geometry of the particle system, we concentrate on the boundary layer in the vicinity of $s = 0$. We begin by considering a continuum ansatz, which we assume to be valid when $i = \mathrm{ord}(n^{\beta})$ for some $0 < \beta \leq \frac{1}{a}$, and which takes the form

$$x(i) = n^{\beta - 1}\hat{\xi}(in^{-\beta}; n), \tag{22}$$

where $\hat{\xi}(\hat{s}; n)$ is again a continuum ansatz with the smoothness and monotonicity properties described before:

($\hat{\xi}$-Smooth) $\hat{\xi} \in C^3[0, \infty)$;
($\hat{\xi}$-Mon) $\hat{\xi}'$ is positive and uniformly bounded away from zero, so that $\hat{\xi}'(\hat{s}) \geq \hat{M} > 0$ for some constant $\hat{M}$.

The choice of scaling in (22) is based on two observations. Firstly, the fact that we propose a new ansatz that is valid when $i = \mathrm{ord}(n^{\beta})$ means that $\hat{\xi}$ must be a function of $\hat{s} := in^{-\beta}$, which is $\mathrm{ord}(1)$ when $i = \mathrm{ord}(n^{\beta})$. Secondly, from $\xi(s) \sim s$ as $s \to 0$, we obtain that $x(i) \sim in^{-1}$ as i decreases out of the region where the bulk ansatz is valid. By the principles that underly the method of matched asymptotic expansions, this must be identical to the behaviour of the rescaled $x(i)$ in (22) as i increases out of the region where this boundary layer ansatz is valid. By scaling $x(i)$ with n^{β} in (22), we can satisfy this requirement by imposing the following matching condition on the leading order solution to $\hat{\xi}(\hat{s})$, based on Van Dyke's matching principle:

$$\hat{\xi}_0(\hat{s}) \sim \hat{s}, \quad \text{as } \hat{s} \to \infty.$$

Now, we proceed by considering the case where $i = \mathrm{ord}(n^\beta)$ and so $\hat{s} = \mathrm{ord}(1)$, and we define $\hat{F}(\hat{s})$ in a similar manner to (17) as follows:

$$\hat{F}(\hat{s}) := \sum_{k=1}^{\lfloor K - sn^\beta \rfloor} V'\big(n^\beta\big[\hat{\xi}(\hat{s}+kn^{-\beta}) - \hat{\xi}(\hat{s})\big]\big) - \sum_{k=1}^{\lfloor sn^\beta \rfloor} V'\big(n^\beta\big[\hat{\xi}(\hat{s}) - \hat{\xi}(\hat{s}-kn^{-\beta})\big]\big) + \sum_{k=K+1}^{n} V'\big(n\big[\xi(0+kn^{-1}) - n^{\beta-1}\hat{\xi}(\hat{s})\big]\big), \quad (23)$$

where K is chosen so that $n^\beta \ll K \ll n$, so that K lies in the intermediate region between the two scaling regimes.

We start by showing that the third term in (23) is small. Using **(Dec)** and **($\hat{\xi}$-Mon)**, we quickly see that

$$V'\big(n\big[\xi(0+kn^{-1}) - n^{\beta-1}\hat{\xi}(\hat{s})\big]\big) = O(K^{-a-1}),$$

which when summed, gives

$$\sum_{k=K+1}^{n} V'\big(n\big[\xi(0+kn^{-1}\big) - n^{\beta-1}\hat{\xi}(\hat{s})\big]\big) = O(K^{-a}) = o(n^{-a\beta}).$$

Moreover, we can manipulate the first two sums in (23) as we did in Section 2.2 by introducing $\hat{H}$ where $n^{\frac{\beta}{a}} \ll \hat{H} \ll n^\beta$, so that

$$\hat{F}(\hat{s}) = \sum_{k=1}^{\hat{H}} \Big[V'\big(n^\beta\big[\hat{\xi}(\hat{s}+kn^{-\beta}) - \hat{\xi}(\hat{s})\big]\big) - V'\big(n^\beta\big[\hat{\xi}(\hat{s}) - \hat{\xi}(\hat{s}-kn^{-\beta})\big]\big)\Big] + \sum_{k=1}^{\lfloor K - \hat{s}n \rfloor - \hat{H}} V'\big(n^\beta\big[\hat{\xi}(\hat{s}+\hat{H}n^{-\beta}+kn^{-\beta}) - \hat{\xi}(\hat{s})\big]\big) - \sum_{k=1}^{\lfloor \hat{s}n \rfloor - \hat{H}} V'\big(n^\beta\big[\hat{\xi}(\hat{s}) - \hat{\xi}(\hat{s}-\hat{H}n^{-\beta}-kn^{-\beta})\big]\big) + o(n^{-\beta}).$$

With $\hat{F}(\hat{s})$ in this form, we can repeat the computations in Section 2.2, ultimately obtaining the result that

$$\hat{F}(\hat{s}) = n^{-\beta}\hat{\xi}''(\hat{s}) \sum_{k=1}^{\infty} \big(V''\big[\hat{\xi}'(\hat{s})k\big]k^2\big) + o(n^{-\beta}),$$

which is similar to (18). Since $\hat{F}(\hat{s}) = 0$ whenever $\hat{s} = in^{-\beta}$ for $i = \mathrm{ord}(n^\beta)$, we again obtain that $\hat{\xi}''(\hat{s}) = 0$. Hence, the leading order behaviour of $\hat{\xi}$ in the proposed boundary layer is identical to the leading order behaviour of ξ. Since there is no qualitative difference between the equation to be solved in the bulk and the equation to be solved in the boundary layer, we conclude that this is not a distinguished limit of the system, and thus the only possible boundary layer in our system is the discrete boundary layer that could occur when $i = \mathrm{ord}(1)$.

2.4 Discrete boundary layer scaling

Having established that there can be no boundary layers associated with a continuum rescaling, we propose the discrete boundary layer ansatz, $nx(i;n) = \chi(i;n)$, where $\chi(i;n)$ is expanded as an asymptotic series in powers of n. As before, we omit the explicit dependence on n unless we wish to emphasise that $\chi(i)$ is an asymptotic series. Since $\chi(i)$ only takes integer arguments, we do not make any smoothness assumptions about $\chi(i)$. To preserve the ordering of the particles, we require that $\chi(i)$ is strictly increasing.

Using Van Dyke's matching principle, we find that the leading order behaviour of $\chi(i)$ for large i must be given by

$$\chi_0(i) \sim i \quad \text{as } i \to \infty.$$

More specifically, we can use Van Dyke's matching principle to match between $\xi'(s)$ and $\chi(i) - \chi(i-1)$, which gives the following, stronger condition on $\chi_0(i)$ as $i \to \infty$:

$$\chi_0(i) - \chi_0(i-1) \sim 1 \quad \text{as } i \to \infty. \tag{24}$$

Let $i = \mathrm{ord}(1)$ and let K be chosen so that $1 \ll K \ll n$. Similar to (16) and (17), we write the force balance equation for the ith particle as:

$$0 = \sum_{\substack{k=0 \\ k\neq i}}^{K} V'\big[\chi(i) - \chi(k)\big] - \sum_{k=K+1}^{n} V'\big(n\big[\xi(kn^{-1}) - n^{-1}\chi(i)\big]\big). \tag{25}$$

By the same method as discussed in Section 2.3, we note that

$$\sum_{k=K+1}^{n} V'\big(n\big[\xi(kn^{-1}) - n^{-1}\chi(i)\big]\big) = O(K^{-a}) = o(1),$$

while the first sum in (25) has no explicit dependence on n except through the fact that χ is an asymptotic series.

Since $\chi_0(i) \sim i$ as $i \to \infty$, we note that the first sum in (25) must be finite as $K \to \infty$. Hence, we can take n and K to ∞ in (25) to obtain the leading order equation

$$0 = \sum_{\substack{k=0 \\ k\neq i}}^{\infty} V'\big[\chi_0(i) - \chi_0(k)\big], \quad i = 1,2,3,\ldots,$$

which must be solved subject to the matching condition in (24). Note that this system of discrete equations generalises those of [20] to a wide class of potentials V.

3 Formal asymptotic analysis – Summary of higher order analysis for $V(x) = |x|^{-a}$

In addition to the leading order results described above, we can use formal asymptotic analysis to determine higher order corrections to the particle positions in the specific case where the potential is given by $V(x) = |x|^{-a}$ for any $a > 1$. In this section, we summarise the main results of this analysis; the technical details can be found in Appendix A. As in §2, we obtain our solutions by assuming a continuum ansatz for the particle positions in the bulk of the of the domain and a discrete ansatz in the boundary layers at the ends of the domain. Using the method of matched asymptotic expansions, we obtain asymptotic solutions to the

particle positions up to $o(n^{-(a-1)})$ in both the bulk problem and the rescaled boundary layer problem.

To obtain equations for the particle positions in the bulk, we draw on the results from [39] to use Euler–Maclaurin summation to express the total force on any particle as the sum of a 'local contribution' involving the particle density at that point, and a singular integral that represents the effect of long-range interactions between particles. At leading order, the particle density is governed by a simple differential equation as in §2. Only at higher orders does the nonlocal effect of the long-range interactions on the bulk behaviour become significant, appearing through a singular integral term.

As previously, we find that the particle positions in the boundary layers are governed by different equations from the particle positions in the bulk. In order to analyse this, we apply the method of matched asymptotic expansions, using the techniques of intermediate matching (see, for example, [21]). This enables us to exploit the existence of an 'intermediate scaling regime', where the bulk ansatz and the boundary layer ansatz give equivalent results, in order to determine the sizes of the asymptotic correction terms and the appropriate matching conditions that relate the bulk solution to the boundary layer solution.

We find that the particle locations in the bulk region are given by $x(i;n) \sim \xi(in^{-1};n)$, where the asymptotic expansion of $\xi(s;n)$ takes different forms depending on the value of a. In the case where $1 < a < 2$, we find that $\xi(s;n)$ takes the form

$$\xi(s;n) = s + \frac{s^{-(a-2)} - (1-s)^{-(a-2)} + 1 - 2s}{\zeta(a)(a-2)(a^3-a)} \frac{1}{n^{a-1}} + o\left(\frac{1}{n^{a-1}}\right); \tag{26a}$$

in the case where $a = 2$, we find that $\xi(s;n)$ takes the form

$$\xi(s;n) = s + \frac{2s-1}{\pi^2} \frac{\log n}{n} + \left[\frac{\log(1-s) - \log(s)}{\pi^2} + (s - \tfrac{1}{2})\tilde{p}\right] \frac{1}{n} + o\left(\frac{1}{n}\right); \tag{26b}$$

and in the case where $a > 2$, we find that

$$\xi(s;n) = s + \sum_{k=1}^{\lceil a-2 \rceil} (s - \tfrac{1}{2}) p_k \frac{1}{n^k} + \left[\frac{s^{-(a-2)} - (1-s)^{-(a-2)}}{\zeta(a)(a-2)(a^3-a)} + (s - \tfrac{1}{2})\tilde{p}\right] \frac{1}{n^{a-1}} + o\Big(\frac{1}{n^{a-1}}\Big), \tag{26c}$$

where $\zeta(s)$ is the Riemann zeta function, and where p_k and $\tilde{p}$ are constants. The constants p_k and $\tilde{p}$ are chosen so that the bulk solution and the boundary layer solution are equivalent in some overlap region. As such, these constants depend on the solutions of the boundary layer problems, and can be defined iteratively as we discuss below.

In the boundary layer, we find that the particle locations are given by $x(i) = n^{-1}\chi(i;n)$, where the expansion of $\chi(i;n)$ takes the form

$$\chi(i;n) = \begin{cases} \displaystyle\sum_{j=0}^{\lceil a-2 \rceil} n^{-j}\chi_j(i) + n^{-(a-1)}\tilde{\chi}(i) + o(n^{-(a-1)}), & a \neq 2; \\ \chi_0(i) + n^{-1}\log n \tilde{\chi}^*(i) + n^{-1}\tilde{\chi}(i) + o(n^{-1}), & a = 2. \end{cases} \tag{27}$$

The sequences χ_j, $\tilde{\chi}$ and $\tilde{\chi}^*$ are found by solving infinite systems. We leave their precise description to Appendix A. The infinite system satisfied by $\chi_j(i)$ is linear for $j \geq 1$, and nonlinear for $j = 0$. These infinite systems must be solved subject to a matching condition with the bulk. For example, $\chi_0(i)$ must satisfy the matching condition given by $\chi_0(i) - \chi_0(i-1) \to 1$ as $i \to \infty$. In the case where $a > 2$, we then obtain p_1 from the limit

$$p_1 = 2 \lim_{i \to \infty} [i - \chi_0(i)],$$

and we find that $\chi_1(i)$ must satisfy the matching condition $\chi_1(i)-\chi_1(i-1)\to p_1$. If $a>3$, we can then define p_2 by the limit

$$p_2 = 2\lim_{i\to\infty}\left[p_1 i-\chi_1(i)\right],$$

and we find that $\chi_2(i)$ must satisfy the matching condition $\chi_2(i)-\chi_2(i-1)\to p_2$. This iterative process can be continued until the $O(n^{-(a-1)})$ terms—or, if $a=2$, $O(n^{-1}\log n)$ terms—are reached. At this stage, we can again use the same process to find the matching conditions for $\tilde{\chi}$ and $\tilde{\chi}^*$. If $a=2$, we find that $\tilde{\chi}^*$ satisfies $\tilde{\chi}^*(i)-\tilde{\chi}^*(i-1)\to\frac{2}{\pi^2}$, while for all $a>1$ we find that $\tilde{\chi}$ satisfies $\tilde{\chi}(i)-\tilde{\chi}(i-1)\to\tilde{p}$, where $\tilde{p}$ is given by

$$\tilde{p}=\begin{cases}-\frac{2}{\zeta(a)(a-2)(a^3-a)}, & a\notin\mathbb{N};\\ 2\lim_{i\to\infty}\left[i-\chi_0(i)\right], & a=2;\\ 2\lim_{i\to\infty}\left[p_{a-1}i-\chi_{a-1}(i)\right]-\frac{2}{\zeta(a)(a-2)(a^3-a)}, & a=3,4,\ldots.\end{cases}$$

One valuable feature of the matched asymptotic analysis is that it gives us more precise details of the decay rates of the discrete solutions, $\chi_k(i)$, than could be obtained for $\chi_0(i)$ using leading order analysis. In particular, we find that the asymptotic behaviour of $\chi_0(i)$ for large i is given by

$$\chi_0(i)=\begin{cases}i+\frac{i^{-(a-2)}}{\zeta(a)(a-2)(a^3-a)}+o\left(i^{-(a-2)}\right), & a<2;\\ i-\frac{\log i}{\pi^2}-\frac{\tilde{p}}{2}+o(1), & a=2;\\ i-\frac{p_1}{2}+\frac{i^{-(a-2)}}{\zeta(a)(a-2)(a^3-a)}+o\left(i^{-(a-2)}\right), & a>2.\end{cases}\tag{28}$$

It follows in all cases that

$$\chi_0(i)-\chi_0(i-1)=1-\frac{i^{-(a-1)}}{\zeta(a)(a^3-a)}+o\big(i^{-(a-1)}\big),\qquad a>1,\tag{29}$$

where the scaling of the error term is implied by the postulated differentiability of ξ.

Similarly, we can obtain bounds on the decay rates of the higher order corrections, $\chi_j(i)$, in the case where $0<j<a-1$. These take the form

$$\chi_j(i)=\begin{cases}p_j i-\frac{p_{j+1}}{2}+O\big(i^{-(a-2-j)}\big), & 0<j<a-2;\\ p_j i-\left(\frac{1}{\zeta(a)(a-2)(a^3-a)}+\frac{\tilde{p}}{2}\right)+o(1), & j=a-2;\\ p_j i+O\big(i^{-(a-2-j)}\big), & a-2<j<a-1.\end{cases}$$

Even higher order corrections to the solution (both in the bulk and in the boundary layer) could potentially be obtained by applying the same asymptotic techniques. However, this would involve addressing the direct influence of the boundary layer on the bulk, leading to significant mathematical complications without leading to greater insights into the behaviour of the solution. In Appendix A we discuss how higher order corrections might be obtained, but we do not pursue any high-order analysis in detail.

Additionally, the results obtained for ξ and χ up to $\mathrm{ord}(n^{-(a-1)})$ can be extended to a larger class of potentials V which satisfy, in addition to **(Reg)**, **(Sing)**, and **(Cvx)**, that

$$V^{(r)}(x)\sim(-1)^r a\cdot(a+1)\cdots(a+r-1)x^{-a-r},\quad \text{as } x\to\infty,\quad \text{for } r=0,\ldots,2\left\lfloor\tfrac{a+3}{2}\right\rfloor.\tag{30}$$

In this general case, we find that many results hold with minor modifications. For example, we find that (29) generalises to

$$\chi_0(i) - \chi_0(i-1) = 1 - \frac{i^{-(a-1)}}{Z(V)(a-1)} + o\big(i^{-(a-1)}\big), \tag{31}$$

where $Z(V)$ is defined by

$$Z(V) := \sum_{k=1}^{\infty} V''(k)k^2.$$

At the end of each subsection of Appendix A we outline how the argument for $-a$-homogeneous V extends to those potentials that satisfy (30). For clarity of the arguments, however, we only present detailed results for $V(x) = |x|^{-a}$.

In summary, Appendix A describes in detail how higher-order corrections to the particle locations can be obtained using formal asymptotic methods analogous to those used in §2. The principal results of this analysis are the asymptotic expansions for $\xi(s)$ given in (26) and the asymptotic behaviour of $\chi_0(i)$ given in (28). The bulk analysis that leads to (26) makes it possible to determine the positions of particles to high accuracy for large values of n, while the boundary layer analysis that leads to (28) can be used to quantify the increase in density at the boundaries, and thereby estimate the force on the boundaries due to the particles.

4 Asymptotic development of the ground state energy

This section is devoted to the statement, proof and discussion of Theorem 43, which demonstrates Γ–convergence of the functional E_n^1 defined in (5). For an introduction to the method of Γ–convergence, we refer the reader to [4] or [12]. As stated in §1.2, to establish these results we make the stronger decay assumption **(Dec+)** in addition to the basic assumptions detailed in §1.1 throughout this section.

We begin in §4.1 by reformulating the minimisation problem for (5) in terms of the variable ε as introduced in (6). In §4.2, we then establish key estimates used in the proof of our Theorem 43, which is then stated and partially proved in §4.3 (the computationally heavy part of the proof is provided in Appendix B.1). In §4.4 we apply Theorem 43 to prove that solutions to the force balance (2) converge to solutions to the boundary layer equation (9). In §4.5 we then argue that **(Dec+)** is a natural condition for the methods we use here, and that additional ideas are required to obtain a result assuming only **(Dec)**, or a yet weaker decay hypothesis.

4.1 Reformulation

Let $\bar{x}(i) := \frac{i}{n}$ be the equispaced configuration. We reinterpret (6) as

$$\varepsilon(i) := n\big(\big[x(i) - x(i-1)\big] - \big[\bar{x}(i) - \bar{x}(i-1)\big]\big) \qquad \text{for } i = 1, \dots, n.$$

Figure 5 illustrates the definition of $\varepsilon(i)$ as the difference between the blown–up perturbations of the positions $x(i)$ relative to the reference equispaced configuration $\bar{x}(i)$ for $i = 0, \dots, n$. We interpret $\varepsilon(i)$ as a strain variable, since it expresses the local change in distance between particles away from the equispaced configuration. Since $x(0) = 0$, the inverse transformation is given by $x(i) = \frac{1}{n}[i + \sum_{j=1}^{i} \varepsilon(i)]$, and we obtain $\sum_{i=1}^{n} \varepsilon(i) = nx(n) - n = 0$.

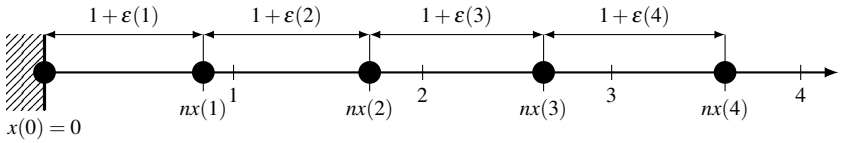

Fig. 5 Zoom-in of the particle system from Figure 1 at the boundary layer. Both choices of variables given by $nx(i)$ and $\varepsilon(i)$ are illustrated.

Expressing the energy difference E_n^1 in (5) in ε, we obtain

$$E_n^1(\varepsilon) := \sum_{k=1}^{n}\sum_{j=0}^{n-k}\left[V\left(k+\sum_{l=j+1}^{j+k}\varepsilon(l)\right)-V(k)\right], \quad \mathrm{Dom}\,E_n^1 = \left\{\varepsilon\in[-1,n]^n \,\middle|\, \varepsilon\cdot\mathbf{1}=0\right\}. \tag{32}$$

We note that the double sum over $V(k)$ equals $E_n(\bar{x})$. We make three basic observations:

1. Since the change of variable given above is a bijection from $\mathscr{D}_n$ to $\mathrm{Dom}\,E_n^1$ and E_n has a unique minimiser in the interior of $\mathscr{D}_n$, it follows that E_n^1 has a unique minimiser in the interior of $\mathrm{Dom}\,E_n^1$.
2. Viewing ε as the perturbation to the distances between particles away from unit spacing, we expect $\varepsilon(i)\approx 0$ for $i\approx\frac{n}{2}$, which is equivalent to the fact that far from the boundary, the distances between particles are close to 1.
3. By the symmetry in the geometry of the double pile-up, the minimiser of E_n^1 has *reversal symmetry*, i.e. $\varepsilon(i)=\varepsilon(n+1-i)$. The reversal symmetry of the minimiser is easily proved from the strict convexity of E_n. We introduce the following notation for 'reversing' a sequence:

$$\text{for } \varepsilon\in\mathrm{Dom}\,E_n^1,\ \text{let } \hat{\varepsilon}(i) := \varepsilon(n+1-i). \tag{33}$$

It is easy to check that $\hat{\varepsilon}\in\mathrm{Dom}\,E_n^1$, and that $E_n^1(\hat{\varepsilon})=E_n^1(\varepsilon)\geq E_n^1((\varepsilon+\hat{\varepsilon})/2)$.

4.2 Structure of E_n^1 and key estimates

In order to prove a Γ–convergence result, we extend the definition of E_n^1 so that these functionals are defined over the same topological space. Here, the right space turns out to be $\ell^2(\mathbb{N})$.

To do so, we define the embedding $\iota_n : \mathrm{Dom}\,E_n^1 \to \ell^2(\mathbb{N})$, where

$$\iota_n\varepsilon(i) := \begin{cases}\varepsilon(i) & \text{if } i=1,\dots,n,\\ 0 & \text{otherwise.}\end{cases}$$

This permits us to extend E_n^1 over $\ell^2(\mathbb{N})$ in the following manner:

$$E_n^1(\varepsilon) = \begin{cases}E_n^1(\varepsilon) & \text{if } \varepsilon\in\iota_n(\mathrm{Dom}\,E_n^1),\\ +\infty & \text{otherwise.}\end{cases}$$

To expose the locally quadratic structure of $E_n^1(\varepsilon)$ as defined in (32), we rewrite it by subtracting and adding a term which is linear in ε. For any $\varepsilon \in \ell^2$ with finite energy, we obtain

$$E_n^1(\varepsilon) = \sum_{k=1}^{n}\sum_{j=0}^{n-k}\left(V\left(k+\sum_{l=j+1}^{k+j}\varepsilon(l)\right) - V(k) - V'(k)\sum_{l=j+1}^{k+j}\varepsilon(l)\right) + \sum_{k=1}^{n}V'(k)\sum_{j=0}^{n-k}\sum_{l=j+1}^{k+j}\varepsilon(l)$$
$$= \underbrace{\sum_{k=1}^{n}\sum_{j=0}^{n-k}\phi_k\left(\sum_{l=j+1}^{k+j}\varepsilon(l)\right)}_{=:Q_n(\varepsilon)} + \left(\sigma^n, \varepsilon+\hat{\varepsilon}\right)_{\ell^2(\mathbb{N})}, \quad (34)$$

where $\phi_k(y) = V(k+y) - V(k) - V'(k)y$ is defined in (8) and

$$\sigma^n(i) := \begin{cases} \sum_{k=i+1}^{n-i}\left[(k-i)\wedge(n-i+1-k)\right]\left|V'(k)\right|, & \text{if } i \le \lfloor n/2\rfloor. \\ 0, & \text{otherwise.} \end{cases} \quad (35)$$

The second equality in (34) follows from changing the order of summations and using the fact that $(\varepsilon, \mathbf{1})_{\ell^2(\mathbb{N})} = 0$; the details of this computation are provided in Appendix B.2. The function ϕ_k is the error of the first order Taylor expansion of $V(x)$ around $x = k$, expressed in the shifted variable $y := x - k$. We interpret σ^n as a stress which arises due to the constraint that the particles are confined to lie in a finite interval.

Lemma 41 states precisely what we mean by Q_n being 'locally quadratic'; it provides a quadratic lower and upper bound for ϕ_k. Both bounds are essential in the proof of Theorem 43. Figure 6 illustrates ϕ_k together with the lower and upper bound. The proof of Lemma 41 is a direct consequence of **(Cvx)**, i.e. the strict convexity of V.

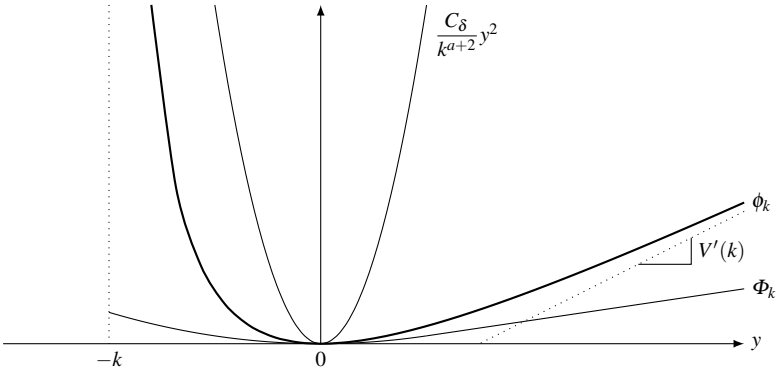

Fig. 6 The function ϕ_k as defined in Lemma 41.

Lemma 41 (Lower bound on V) *For any $k \in [1,+\infty)$, it holds for all $y \in (-k,+\infty)$ that*

$$\phi_k(y) \ge \Phi_k(y) := \begin{cases} \frac{1}{2}\lambda(k+1)y^2 & y \in (-k,1], \\ \lambda(k+1)\left(y-\frac{1}{2}\right) & y \in [1,+\infty). \end{cases}$$

Moreover, if $y \ge k(\delta-1)$ for some $\delta > 0$, then there exists a $C_\delta > 0$ such that $\phi_k(y) \le C_\delta k^{-a-2}y^2$.

Proof The proof relies on the following observation. For any $f, g \in C^2(\mathbb{R})$ satisfying $f(0) = g(0)$, $f'(0) = g'(0)$, and $f'' \geq g''$ on some interval $I \ni 0$, then $f \geq g$ on I. This is easily proven from the fact that $f - g$ is convex with $0 = (f-g)(0) = (f-g)'(0)$.

Since $V(x)$ is $\lambda(x)$-convex in the sense of **(Cvx)**, it follows that $\phi_k(y)$ is $\lambda(y+k)$-convex. Since λ is decreasing, the lower bound of ϕ_k in Lemma 41 follows.

Since $V \in C^2(0,\infty)$ and $V''(x) \lesssim 1/x^{a+2}$, it holds that

$$\sup_{y > k(\delta-1)} \phi_k''(y) = \sup_{x > k\delta} V''(x) \leq \frac{2C}{(\delta k)^{a+2}}$$

is finite for any fixed $\delta > 0$. The upper bound for ϕ_k follows.

The linear term in (34) is fully characterized by σ^n. Lemma 42 states its key properties. Its proof relies on the decay property $|V'(x)| \lesssim x^{-a-1}$ in (1) with $a > 3/2$; in fact, this is the key point at which the assumption **(Dec+)** is necessary for our continuing analysis.

Lemma 42 (Properties of σ^n) *$\sigma^n \in \ell^2(\mathbb{N})$ as defined in* (35) *satisfies*

$$0 \leq \sigma^n(i) \leq \sigma^\infty(i) = \sum_{k=i+1}^{\infty} (k-i)\big|V'(k)\big|, \quad \textit{for all } i \geq 1. \tag{36}$$

Moreover, $\sigma^n \to \sigma^\infty$ in $\ell^2(\mathbb{N})$ as $n \to \infty$.

Proof (36) follows from the definitions viz.

$$\sigma^n(i) \leq \sum_{k=i+1}^{n-i} (k-i)\big|V'(k)\big| \leq \sum_{k=i+1}^{\infty} (k-i)\big|V'(k)\big| = \sigma^\infty(i). \tag{37}$$

For the convergence in $\ell^2(\mathbb{N})$, we set $R_n := \lfloor n/2 \rfloor$ and note that the summands in (35) and (36) are equal for $k = i+1, \ldots, R_n$. Since $a > 3/2$ and the decay property $|V'(x)| \lesssim x^{-a-1}$ in (1), we obtain the convergence from

$$\begin{aligned}
\big\|\sigma^\infty - \sigma^n\big\|_{\ell^2(\mathbb{N})}^2 &\leq \sum_{i=1}^{R_n-1} \left(\sum_{k=R_n+1}^{\infty} (k-i)\big|V'(k)\big| \right)^2 + \sum_{i=R_n}^{\infty} \left(\sum_{k=i+1}^{\infty} (k-i)\big|V'(k)\big| \right)^2 \\
&\lesssim \sum_{i=1}^{R_n-1} \left(\int_{R_n}^{\infty} \frac{x-i}{x^{a+1}} \mathrm{d}x \right)^2 + \sum_{i=R_n}^{\infty} \left(\sum_{k=i+1}^{\infty} k \frac{1}{k^{a+1}} \right)^2 \\
&\lesssim \sum_{i-1}^{R_n-1} \frac{(R_n-i)^2}{R_n^{2a}} + \sum_{i=R_n}^{\infty} \frac{1}{i^{2(a-1)}} \lesssim \frac{1}{n^{2a-3}} \xrightarrow{n\to\infty} 0.
\end{aligned}$$

4.3 Main result: Γ–convergence

We prove Γ–convergence in the weak topology of $\ell^2(\mathbb{N})$. To accommodate for a splitting of $\varepsilon^n \in \mathrm{Dom}\, E_n^1$ to account for the boundary layer at the left and right barrier separately, we introduce the following notation:

$$\varepsilon^{n,1/2}(i) := \begin{cases} \varepsilon^n(i) & \text{if } i = 1, \ldots, \lceil n/2 \rceil, \\ 0 & \text{otherwise,} \end{cases} \quad \text{and} \quad \hat{\varepsilon}^{n,1/2}(i) := \begin{cases} \hat{\varepsilon}^n(i) & \text{if } i = 1, \ldots, \lceil n/2 \rceil, \\ 0 & \text{otherwise,} \end{cases}$$

We will also write

$$\varepsilon^n \xrightarrow{2} (\varepsilon,\hat{\varepsilon}) \Leftrightarrow \left\{ \begin{array}{l} \varepsilon^{n,1/2} \to \varepsilon \\ \hat{\varepsilon}^{n,1/2} \to \hat{\varepsilon} \end{array} \right\} \text{ in } \ell^2(\mathbb{N}), \quad \text{and} \quad \varepsilon^n \xrightarrow{2}_{\rightharpoonup} (\varepsilon,\hat{\varepsilon}) \Leftrightarrow \left\{ \begin{array}{l} \varepsilon^{n,1/2} \rightharpoonup \varepsilon \\ \hat{\varepsilon}^{n,1/2} \rightharpoonup \hat{\varepsilon} \end{array} \right\} \text{ in } \ell^2(\mathbb{N}). \tag{38}$$

We remark that the reversal of a sequence (33) is only well-defined for sequences that are equivalent to finite dimensional vectors (i.e. sequences which have finite support). Therefore, in the definition above, there need not be any relation between ε and $\hat{\varepsilon}$, while $\hat{\varepsilon}^n(i) = \varepsilon^n(n+1-i)$.

Theorem 43 states that the Γ–limit of E_n^1 is given by

$$\begin{aligned} \operatorname{Dom} E_\infty^1 &:= \big\{ (\varepsilon,\hat{\varepsilon}) \in \ell^2(\mathbb{N}) \times \ell^2(\mathbb{N}) \,\big|\, \varepsilon(i), \hat{\varepsilon}(i) \geq -1 \ \forall i \geq 1 \big\}, \\ E_\infty^1(\varepsilon,\hat{\varepsilon}) &:= \underbrace{\sum_{k=1}^{\infty} \sum_{j=0}^{\infty} \phi_k\Big(\sum_{l=j+1}^{k+j} \varepsilon(l) \Big)}_{=:Q_\infty} + \underbrace{\sum_{k=1}^{\infty} \sum_{j=0}^{\infty} \phi_k\Big(\sum_{l=j+1}^{k+j} \hat{\varepsilon}(l) \Big)}_{=:\hat{Q}_\infty} + \big(\sigma^\infty, \varepsilon + \hat{\varepsilon}\big)_{\ell^2(\mathbb{N})}, \end{aligned} \tag{39}$$

where ϕ_k as in (8) and σ^∞ as in (36).

Theorem 43 (Γ–convergence of E_n^1) *If $E_n^1(\varepsilon^n)$ is uniformly bounded in n for some sequence $(\varepsilon^n) \subset \ell^2(\mathbb{N})$, then $\|\varepsilon^n\|_{\ell^2}$ is uniformly bounded. Moreover, for any $(\varepsilon,\hat{\varepsilon}) \in \operatorname{Dom} E_\infty^1$, it holds that*

$$\text{for all } \varepsilon^n \xrightarrow{2}_{\rightharpoonup} (\varepsilon,\hat{\varepsilon}) \text{ with } \varepsilon^n \in \operatorname{Dom} E_n^1, \qquad \liminf_{n\to\infty} E_n^1(\varepsilon^n) \geq E_\infty^1(\varepsilon,\hat{\varepsilon}), \tag{40a}$$

$$\text{there exists } \varepsilon^n \xrightarrow{2} (\varepsilon,\hat{\varepsilon}) \text{ with } \varepsilon^n \in \operatorname{Dom} E_n^1 \text{ such that} \quad \limsup_{n\to\infty} E_n^1(\varepsilon^n) \leq E_\infty^1(\varepsilon,\hat{\varepsilon}). \tag{40b}$$

The main novelty in the proof of Theorem 43 is the argument leading to the compactness. The proofs of the inequalities (40a) and (40b) follow from a more standard approach, and are therefore left until Appendix B.1.

Proof (Proof of compactness in Theorem 43) First we obtain a sufficient lower bound on Q_n in (34). we use Lemma 41 on the nearest neighbour interactions to estimate

$$Q_n(\varepsilon^n) = \sum_{k=1}^{n} \sum_{j=0}^{n-k} \phi_k\Big(\sum_{l=j+1}^{k+j} \varepsilon(l) \Big) \geq \sum_{j=1}^{n} \Phi_1\big(\varepsilon(j)\big). \tag{41}$$

To obtain a sufficient lower bound of $E_n^1(\varepsilon^n)$ from (41), (37) and $\sigma^\infty \in \ell^2(\mathbb{N})$, we split ε^n into a positive and negative part viz.

$$\varepsilon_+^n(i) := \varepsilon^n(i) \vee 0 \geq 0, \qquad \varepsilon_-^n(i) := -\big(\varepsilon^n(i) \wedge 0\big) \geq 0.$$

Then, we use Lemma 41 and $\Phi_1(0) = 0$ to estimate

$$\begin{aligned}
E_n^1(\varepsilon^n) &\geq \sum_{j=1}^{n} \phi_1\big(\varepsilon^n(j)\big) + \big(\sigma^n, \varepsilon_+^n + \hat{\varepsilon}_+^n\big)_{\ell^2(\mathbb{N})} - \big(\sigma^n, \varepsilon_-^n + \hat{\varepsilon}_-^n\big)_{\ell^2(\mathbb{N})} \\
&\geq \sum_{j=1}^{n} \Big[\Phi_1\big(\varepsilon_+^n(j)\big) + \Phi_1\big(-\varepsilon_-^n(j)\big)\Big] - \sum_{j=1}^{n} \sigma^\infty(j)\big(\varepsilon_-^n(j) + \hat{\varepsilon}_-^n(j)\big) \\
&\geq \sum_{j=1}^{n} \Phi_1\big(\varepsilon_+^n(j)\big) + \tfrac{\lambda(2)}{4} \sum_{j=1}^{n} \Big[\varepsilon_-^n(j)^2 + \big(\hat{\varepsilon}_-^n(j)\big)^2\Big] - \sum_{j=1}^{n} \sigma^\infty(j)\big(\varepsilon_-^n(j) + \hat{\varepsilon}_-^n(j)\big) \\
&= \sum_{j=1}^{n} \Phi_1\big(\varepsilon_+^n(j)\big) + \tfrac{\lambda(2)}{4} \sum_{j=1}^{n} \Big[\big(\varepsilon_-^n(j) - \tfrac{2\sigma^\infty(j)}{\lambda(2)}\big)^2 + \big(\hat{\varepsilon}_-^n(j) - \tfrac{2\sigma^\infty(j)}{\lambda(2)}\big)^2\Big] \\
&\quad - \tfrac{2}{\lambda(2)} \sum_{j=1}^{n} \sigma^\infty(j)^2 \\
&\geq \sum_{j=1}^{n} \Phi_1\big(\varepsilon_+^n(j)\big) + c\,\big\|\,\varepsilon_-^n - \tfrac{2}{\lambda(2)}\sigma^\infty\big\|_{\ell^2(\mathbb{N})}^2 + c\,\big\|\,\hat{\varepsilon}_-^n - \tfrac{2}{\lambda(2)}\sigma^\infty\big\|_{\ell^2(\mathbb{N})}^2 - C. \qquad (42)
\end{aligned}$$

Hence, since $E_n^1(\varepsilon^n) \leq C$ by hypothesis, we obtain from $\sigma^\infty \in \ell^2(\mathbb{N})$ that (ε_-^n) and $(\hat{\varepsilon}_-^n)$ are uniformly bounded in $\ell^2(\mathbb{N})$.

It remains to show that (ε_+^n) is uniformly bounded in $\ell^2(\mathbb{N})$. We obtain this from the uniform boundedness of $\sum_{j=1}^n \Phi_1\big(\varepsilon_+^n(j)\big)$ by (42). Indeed, it follows from the linear growth of Φ_1 that for some positive constant C' we have

$$\varepsilon_+^n(i) \leq C' \qquad \text{for all } i = 1, \ldots, n \text{ and all } n \in \mathbb{N}.$$

Hence, there exists a constant c (which depends on C') such that

$$\Phi_1(x) \geq cx^2 \qquad \text{for all } x \in [0, C'],$$

and so

$$E_n^1(\varepsilon^n) \geq c\left(\sum_{j=1}^{n} \big(\varepsilon_+^n(j)\big)^2\right) - C = c\|\varepsilon_+^n\|_{\ell^2}^2 - C,$$

thus implying that (ε_+^n) is uniformly bounded in $\ell^2(\mathbb{N})$.

Remark 44 (Weaker condition on V) *A careful study of the above proof and the one in Appendix B.1 shows that the weaker condition given by $V''(x) < c_\delta |x|^{-a-3/2}$ for any $x \in (\delta, \infty)$ is sufficient as long as* (1) *holds. Since we do not know of an interesting example of an interaction potential which satisfies this weakened version of* **(Dec+)***, we have assumed* **(Dec+)** *for convenience.*

4.4 Properties of the limit energy and the Euler–Lagrange equation

From (7) and (39) we observe that E_∞^1 splits as

$$E_\infty^1(\varepsilon, \hat{\varepsilon}) = E_\infty^l(\varepsilon) + E_\infty^r(\hat{\varepsilon}),$$

where E_∞^l and E_∞^r are identical. This splitting shows that the interaction between the two boundary layers completely decouples as $n \to \infty$. For this reason we focus on E_∞^l in the remainder.

Lemma 45 *Let E^l_∞ and $\mathrm{Dom}\,E^l_\infty$ be defined as in* (7). *E^l_∞ has a unique minimiser, denoted $\bar\varepsilon$, on $\mathrm{Dom}\,E^l_\infty$. Moreover, $\bar\varepsilon \in \mathrm{int}\big(\mathrm{Dom}\,E^l_\infty\big)$.*

Proof We note that E^l_∞ is bounded from below by (42) and (40b). It is not identical to ∞, because $E^l_\infty(0) = 0$.

By the standard properties of Γ–convergence, Theorem 43 implies that the unique minimisers of E^1_n (see Section 4.1) converge to a minimiser of E^1_∞ in $\mathrm{Dom}\,E^1_\infty$. Since E^1_∞ is strictly convex (by the argument that implies the strict convexity of E^1_n in Section 4.1), the minimiser is unique. By the argument at the beginning of the proof of (40b), it follows that $\bar\varepsilon \in \mathrm{int}\big(\mathrm{Dom}\,E^l_\infty\big)$.

To compare the Euler–Lagrange equation with the equation for the boundary layer in (9), we change variables once more. Let u_i be the blown-up perturbation of the particles with respect to the equidistant configuration, i.e.

$$u(i) := \sum_{j=1}^{i} \varepsilon(j), \quad u(0) := 0.$$

This transformation defines a bijection between $\mathrm{Dom}\,E^1_\infty$ and the set of sequences given by

$$\mathscr{U} := \big\{ \big(0, u(1), u(2), \dots\big) \,\big|\, Du \in \ell^2(\mathbb{N}) \text{ and } Du(i) \geq -1 \text{ for all } i \geq 1 \big\},$$

where Du denotes the finite difference

$$Du(i) = u(i) - u(i-1).$$

$\mathscr{U}$ is a subset of the Hilbert space

$$\mathscr{W} := \big\{ \big(0, u(1), u(2), \dots\big) \,\big|\, Du \in \ell^2(\mathbb{N}) \big\} \quad \text{where} \quad (u,v)_{\mathscr{W}} = (Du, Dv)_{\ell^2(\mathbb{N})}.$$

We note that $\mathscr{U}$ is a convex subset of $\mathscr{W}$, and since $\bar\varepsilon$ is in the interior of $\mathrm{Dom}\,E^l_\infty$, it holds that $\bar u$, the image of $\bar\varepsilon$ under this change of variable, is in the interior of $\mathscr{U}$. Therefore, the Euler–Lagrange equation is given by

$$0 = \frac{\partial E^1_\infty(u)}{\partial u(i)}, \quad \text{for all } i \geq 1. \tag{43}$$

By taking the derivative of E^1_∞, a straightforward calculation shows that the constant term in ϕ_k vanishes, and that the linear term of ϕ_k cancels with the linear term involving σ^∞. The explicit form of (43) is given by

$$\begin{cases} 0 = \displaystyle\sum_{\substack{j=0 \\ j\neq i}}^{\infty} V'\big(u(i) - u(j) + i - j\big), \quad \text{for all } i \geq 1, \\ 0 = u(0), \\ Du \in \ell^2(\mathbb{N}). \end{cases} \tag{44}$$

It is easy to see that (44) is equivalent to (9).

4.5 The case $a < 3/2$

Here we motivate why the case $a < 3/2$ is significantly different from Theorem 43. We do this by separating two scenarios; $a \leq 1$ and $1 < a < 3/2$.

Many steps in the proof of Theorem 43 require $a > 1$. The main reason for this requirement is that $a \leq 1$ does not guarantee integrability of the tail of V. Moreover, our choice for the variables given by ε^n relies heavily upon the fact that the particles in the bulk should be equispaced. As remarked above, this was expected due to the results of [31]: these break down when the tail of V fails to be integrable.

The case $1 < a < 3/2$ is more delicate. To illustrate that Theorem 43 does not hold, we show that the functional E^1_∞ is not bounded from below in this case. As a consequence, it would seem that there is a term which has an energy scaling which is neglected in this case, and lies between the bulk energy due to the equispaced configuration and the boundary layer energy. We expect that this term describes a correction to the bulk profile, which appears because the boundary layers begin to interact with each other as the interactions become more nonlocal.

To show that E^1_∞ is not bounded from below when $1 < a < 3/2$, we assume that $V''(x) \simeq x^{-a-2}$ for large x, which implies (by a similar argument leading to (1)) that $|V'(x)| \simeq x^{-a-1}$ and $V(x) \simeq x^{-a}$ for large x. We claim that $\sigma^\infty_i \simeq i^{1-a}$, which implies

$$\sigma^\infty \in \ell^p(\mathbb{N}) \iff p > \frac{1}{a-1}.$$

To prove this claim, we use $V'(x) \simeq x^{-a-1}$ for large x to obtain

$$\sigma^\infty_i = \sum_{k=i+1}^{\infty} (k-i)\big|V'(k)\big| \simeq \sum_{j=1}^{\infty} \frac{j}{(j+i)^{a+1}} \quad \text{for large } i.$$

Then, we estimate from above and below to obtain the desired result:

$$\sigma^\infty_i \lesssim \sum_{j=1}^{\infty} \frac{1}{(j+i)^a} \simeq i^{1-a},$$

$$\sigma^\infty_i \geq \sum_{j=1}^{i} \frac{j}{(2i)^{a+1}} + \sum_{j=i+1}^{\infty} \frac{1/2}{(j+i)^a} \simeq i^{1-a}.$$

Next we estimate $Q_\infty(\varepsilon)$ (i.e. the first term of E^1_∞ as in (39)) from above for $(\varepsilon,\varepsilon) \in \operatorname{Dom} E^1_\infty$ satisfying $-1/2 \leq \varepsilon(i) \leq 0$ for all $i \geq 1$. By first using Lemma 41 and then applying Jensen's inequality, we obtain

$$Q_\infty(\varepsilon) = \sum_{k=1}^{\infty}\sum_{j=0}^{\infty} \phi_k\Big(\sum_{l=j+1}^{k+j} \varepsilon(l)\Big) \lesssim \sum_{k=1}^{\infty}\sum_{j=0}^{\infty} k^{-a-2}k^2\Big(\frac{1}{k}\sum_{l=j+1}^{k+j} \varepsilon(l)\Big)^2$$

$$\leq \sum_{k=1}^{\infty}\sum_{j=0}^{\infty} k^{-a-1} \sum_{l=j+1}^{k+j} \varepsilon(l)^2.$$

By the computations in Appendix B.2 it then follows that

$$Q_\infty(\varepsilon) \lesssim \sum_{j=1}^{\infty} \Big(\sum_{k=1}^{\infty} k^{-a}\Big)\varepsilon_j^2 \simeq \|\varepsilon\|^2_{\ell^2(\mathbb{N})}.$$

It is now easy to find $(\varepsilon,\hat{\varepsilon}) \in \mathrm{Dom}\, E^1_\infty$ for which $E^1_\infty(\varepsilon,\hat{\varepsilon}) = -\infty$. We set $\varepsilon(i) = -i^{-b}/2$ with $1/2 < b < 2-a$ and $\hat{\varepsilon} = \varepsilon$. By these choices, we have

$$(\sigma^\infty, \varepsilon)_{\ell^2(\mathbb{N})} \simeq -\sum_{i=1}^{\infty} i^{1-a} i^{-b} \leq -\sum_{i=1}^{\infty} \frac{1}{i} = -\infty,$$

$$Q_\infty(\varepsilon) \lesssim \sum_{i=1}^{\infty} \frac{1}{i^{2b}} = C,$$

and analogous estimates for $\hat{\varepsilon}$, and thus $E^1_\infty(\varepsilon,\hat{\varepsilon}) = -\infty$.

5 Numerical computations of the solutions to (2) and (9)

In this section, we investigate by means of numerical computations to what extent the solution to the equation for the boundary layer in (9) matches with the solution to the force balance in (2) for several values of n. In §5.1 we describe our numerical method for solving the 'infinite' force balance (9). In §5.2 and §5.3 we compare the solutions of (2) for various values of n to the solution of (9) for respectively two physically–motivated choices of the interaction potential V. In §5.4 we use these solutions to compute the force which the particles exert on the barriers (see (10)–(12)).

5.1 Numerical method for solving equation (9) for the boundary layer

To approximate the infinite sum in (9) by a finite sum which depends on a finite set of unknowns, we assume the particles to be equispaced after a fixed index I, i.e. $\chi(j) = \chi(I) + (j-I)$ for all $j \geq I$. This choice is equivalent to finding the minimiser of E^l_∞ (defined in (7)) in the finite dimensional set $\left\{\varepsilon \in \mathrm{Dom}\, E^l_\infty \,\middle|\, \varepsilon(j) = 0 \text{ for all } j > I\right\}$, and the related force balance can be written as

$$0 = \sum_{\substack{j=0 \\ j\neq i}}^{I} -V'(\chi(i)-\chi(j)) - \sum_{j=I+1}^{\infty} V'(\chi(i)-\chi(I)+I-j), \qquad \forall\, i = 1,\ldots,I. \tag{45}$$

In order to evaluate the infinite sum in (45) numerically, we introduce a second approximation. We use the Euler–Maclaurin summation formula (see, for example, [9]) to approximate the tail of the sum, given by all indices j which are larger than some fixed index $J > I$, with an integral. To this end, we use oddness of V' to rewrite the infinite sum in (45) as

$$\sum_{j=I+1}^{\infty} V'(\chi(i)-\chi(I)+I-j) = \sum_{j=I+1}^{J-1} V'(\chi(i)-\chi(I)+I-j) - \sum_{k=0}^{\infty} V'(\chi(I)-\chi(i)-I+J+k).$$

The Euler–Maclaurin summation formula gives us the result that

$$\sum_{k=0}^{\infty} V'(\chi(I)-\chi(i)+J-I+k) = \int_0^\infty V'(\chi(I)-\chi(i)+J-I+r)\,\mathrm{d}r - \tfrac{1}{2}V'(\chi(I)-\chi(i)+J-I) + R,$$

where the remainder term R is given by (assuming that $V \in C^3([J-I,\infty))$)

$$R := \int_0^\infty \frac{B_2(\{r\})}{2} V'''(\chi(I)-\chi(i)+J-I+r)\,\mathrm{d}r, \tag{46}$$

where $B_2(\{\cdot\})$ is the 1-periodic extension of the second Bernoulli polynomial. If we further assume that $V''' \leq 0$, we can use $\|B_2(\{\cdot\})\|_\infty = \frac{1}{6}$ to estimate

$$|R| \leq \frac{1}{12}\left|\int_0^\infty V'''(\chi(I)-\chi(i)+J-I+r)\,\mathrm{d}r\right| = \frac{1}{12}V''(\chi(I)-\chi(i)+J-I) \lesssim |J-I|^{-a-2}.$$

Depending on the regularity and monotonicity properties of a given V, we can obtain stronger estimates on R by using integration by parts in (46).

Neglecting R, we obtain the following non-linear system of equations from (45):

$$\begin{cases} 0 = -\dfrac{1}{2}V'(\chi(i)-\chi(J)) - V(\chi(i)-\chi(J)) - \displaystyle\sum_{\substack{j=0 \\ j\neq i}}^{J-1} V'(\chi(i)-\chi(j)), & \forall\, i = 1,\dots,I, \\ \chi(j) = \chi(I)+j-I, & \forall\, j = I+1,\dots,J, \\ \chi(0) = 0. \end{cases} \tag{47}$$

While (2) and (47) are both nonlinear systems of respectively n and I unknowns, we wish to highlight the practical benefits of solving (47) rather than (2). First, we expect that I can be chosen much smaller than n without loss of accuracy, since (47) only includes explicitly the boundary effect at the left barrier, whereas (2) also requires to solve for the bulk and the boundary layer at the right barrier. Second, Theorem 43 implies (apart from the error induced by I and J) that the solution to (47), which needs to be computed only once, approximates the boundary layer in the n-dependent solution of (2) for *any* n large enough. Third, our numerical method to approximate the infinite system (9) by (47) is *ad hoc*; we believe that it can be improved in terms of accuracy and computational efficiency by exploiting the boundary condition in (9) in a more sophisticated manner.

5.2 Computations for the homogeneous potential $V_2(x) = x^{-2}$

The potential $V_2(x) = x^{-2}$ is a special case of the setting in [20], and models the interaction between dislocation dipoles. It satisfies all basic assumptions in §1.1, as well as both strengthened hypotheses **(Reg+)** and **(Dec+)** given in §1.2.

Taking $V = V_2$, we compute numerically $x^n \in \mathscr{D}_n$ as the solution to (2) for various values of n, and $\chi(1),\dots,\chi(I)$ as the solution to (47) with $I = 10^3$ and $J - I = 10^2$. We extend χ to a sequence $\chi : \mathbb{N} \to \mathbb{R}$ by setting $\chi(j) = \chi(I) + j - I$ for all $j > I$. Given x^n and χ, we use (6) to define

$$\chi^n(i) := nx^n(i) \quad \text{and} \quad \varepsilon^n(i) := n[x^n(i) - x^n(i-1)] - 1 \tag{48}$$

as alternative representations of x^n, and

$$\varepsilon(i) := \chi(i) - \chi(i-1) - 1 \quad \text{and} \quad x(i;n) := \tfrac{1}{n}\chi(i) \tag{49}$$

as alternative representations of χ. Similar to Figure 3 we define the discrete approximation of the particle density on $[0,1]$ as

$$\rho^n(i) := \frac{2}{\chi^n(i+1)-\chi^n(i-1)} \qquad \text{for all } i = 1,\dots,n-1, \tag{50}$$

$$\rho(i) := \frac{2}{\chi(i+1)-\chi(i-1)} \qquad \text{for all } i = 1,2,\dots, \tag{51}$$

which we represent as piecewise affine functions $\hat{\rho}^n(y)$ and $\hat{\rho}(y)$ for the *microscopic* variable $y \in (0,n)$ by linear interpolation of the sets of grid points given respectively by

$$(\chi^n(i),\rho^n(i))_{i=1}^{n-1} \quad \text{and} \quad (\chi(i),\rho(i))_{i=1}^{\infty}.$$

In addition, we set $\rho^n(x) := \hat{\rho}^n(nx)$ and $\rho(x;n) := \hat{\rho}(nx)$ for the *macroscopic* variable $x \in (0,1)$. We note that the graphs of $\rho^n(x)$ and $\rho(x;n)$ are equal to the linear interpolation of the sets of grid points $(x^n(i),\rho^n(i))_{i=1}^{n-1}$ and $(x(i;n),\rho(i))_{i=1}^{\infty}$.

Figure 7 compares the boundary layer profiles of the solutions to (2) and (47) expressed in the variables ε^n and ε. Since Theorem 43 and Lemma 45 imply that ε^n converges to the exact solution to (9) as $n \to \infty$ in the convergence specified in (38), Figure 7 illustrates that our numerically computed χ is a good approximation of the exact solution to (9).

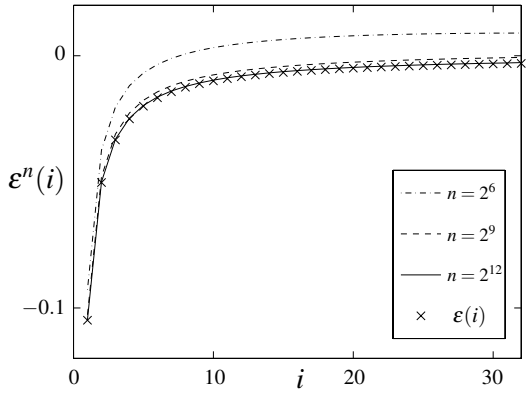

Fig. 7 Comparison between the solutions of (2) and (47) expressed in the variables ε^n (48) and ε (49). The three line plots of $\varepsilon^n(i)$ for $n = 2^6, 2^9, 2^{12}$ illustrate the convergence to ε ($\times$).

Next we test the rate of convergence at which $\varepsilon^n(i)$ converges to $\varepsilon(i)$ as $n \to \infty$ for fixed i. To bypass the dependence of χ on I and J, we consider the incremental error given by

$$d^n(i) := |\varepsilon^n(i) - \varepsilon^{2n}(i)| \quad \text{for } \textit{any} \text{ fixed } i \le \tfrac{n}{2}. \tag{52}$$

Figure 8 illustrates the decay rate of $d^n(i)$. This rate is consistent with (27), which states that $d^n(i) \sim \frac{1}{n}\log n$.

Figure 9.(a) illustrates the discrete densities $\hat{\rho}^n(y)$ and $\hat{\rho}(y)$ (defined below (51)) on the left part of the microscopic domain $y \in [0,n]$. It suggests that χ gives a good approximation of the boundary layer in χ^n for large values of n, and that the size of the boundary layer is $\mathcal{O}(1)$ on the micro-scale. Figure 9.(b) illustrates the corresponding profiles $\rho^n(x)$ and

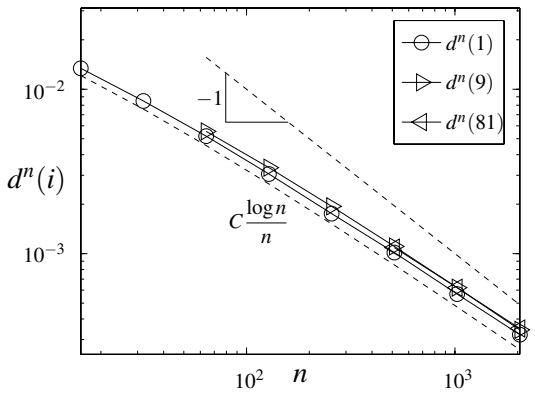

Fig. 8 Given the solutions x^n to (2) for for $n = 2^4, 2^5, \ldots, 2^{12}$, the decay rate of the incremental error $d^n(i)$ (computed from (52) and (48)) is illustrated as a function of n for $i = 1, 9, 81$. The graphs $n \mapsto d^n(i)$ hardly dependent of i; the graphs of $n \mapsto d^n(i)$ for $i = 3, 27$ are omitted since they are visibly indistinguishable from those for $i = 9, 81$. The decay rate of $d^n(i)$ seems similar to $O(n^{-1}\log n)$.

$\rho(x;n)$ on the macroscopic domain $x = \frac{y}{n} \in [0,1]$. We interpret $\rho(x;n)$ as the improvement of the continuum density $\overline{\rho} \equiv 1$ (which is obtained in [31]), which approximates the 'exact' discrete density $\rho^n(x)$ increasingly well as n increases. We note that $\rho(x;n)$ only depends on n through a rescaling; ρ has to be computed only once from (47).

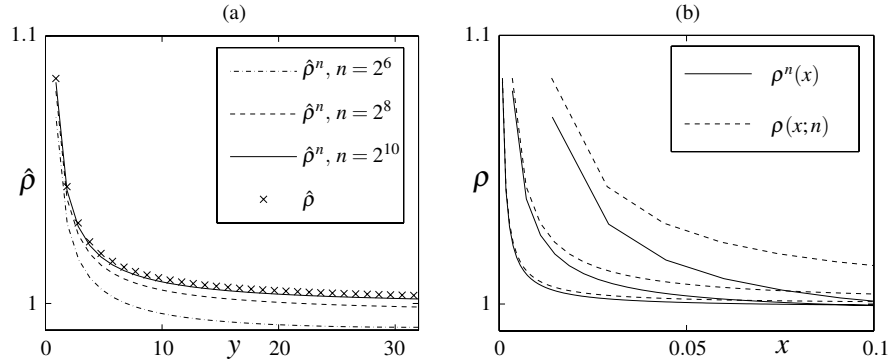

Fig. 9 Comparison between the solutions of (2) and (47) represented respectively by their 'discrete' densities $\hat{\rho}^n$ and $\hat{\rho}$ (see (50), (51) and the paragraph below them) on both: (a) the micro-scale $y \in [0,n]$, and (b) the macro-scale $x = \frac{y}{n} \in [0,1]$. In (b), both the dashed and solid graphs correspond from right to left to $n = 2^6, 2^8, 2^{10}$.

The n-dependent offset between $\hat{\rho}^n$ and $\hat{\rho}$ may be further reduced by computing and solving numerically the higher-order terms $\tilde{\chi}^*$ and $\tilde{\chi}$ in the expansion in (27). It is beyond the scope of this section to pursue this further correction to $\hat{\rho}$.

5.3 Computations for the dislocation wall potential

The potential describing the interaction of dislocation walls [16] is given by

$$V_{\text{wall}}(x) := x\coth x - \log|2\sinh x|. \tag{53}$$

It satisfies all assumptions listed in §1.1, including **(Reg+)** and **(Dec+)** for any $a \in \mathbb{R}$ as defined in §1.2.

We repeat the numerical computation in §5.2 with V_2 replaced by V_{wall}. We compute χ from (47) with $I = 200$ and $J - I = 20$ (the exponential tails of V allow us to take smaller values for I and J without loss of significant accuracy). Figures 10, 11 and 12 are respectively the counterparts of Figures 7, 8 and 9 for V_2 replaced by V_{wall}. Since most observations in §5.2 are similar to those for Figures 10, 11 and 12, we focus on the differences.

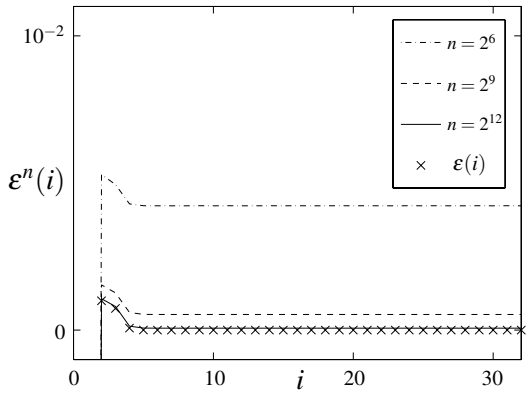

Fig. 10 Same setup as in Figure 7, but here ε^n and ε are computed for $V = V_{\text{wall}}$ instead of V_2. The data for $\varepsilon^n(1)$ are $-O(10^{-1})$, which are relatively far away from the range of the vertical axis.

An intriguing difference with Figure 7 is that the profiles of ε^n and ε in Figure 10 are not monotone. This observation shows that different potentials satisfying our imposed assumptions can result in qualitatively different boundary layer profiles. Moreover, the values of $\varepsilon^n(i)$ and $\varepsilon(i)$ for $i \geq 2$ are an order of magnitude smaller than those obtained in §5.2, and they decay faster to 0 as i increases. This decay is in line with (4).

Figure 11 strongly suggests that the incremental errors $d^n(i)$ defined in (52) decay as n^{-1}. Again, this rate of decay is in line with the theoretical result in (27), even though V_{wall} is not homogeneous.

Figure 12.(b) illustrates a 'dip' in the density profiles of both $\rho^n(x)$ and $\rho(x;n)$. This curious dip corresponds to the non-monotonicity in Figure 10, and was also observed in the boundary layer profiles of [15] which are computed with the same potential V_{wall}, but for a different scaling regime than that in our setting introduced in §1.1.

5.4 Force on the barriers

Given x^n and χ as either computed in §5.2 for $V = V_2$ or in §5.3 for $V = V_{\text{wall}}$, we compute the force which the particles exert on the barrier as given by:

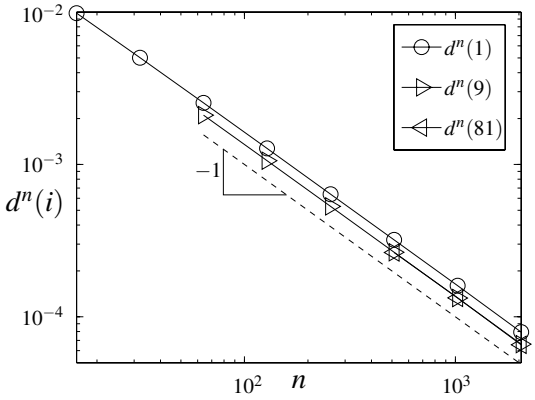

Fig. 11 Same setup as in Figure 8. Here, d^n is computed for $V = V_{\text{wall}}$ instead of V_2. Again, the graphs of $n \mapsto d^n(i)$ for $i = 3, 27$ are visibly indistinguishable from those for $i = 9, 81$, and are therefore omitted.

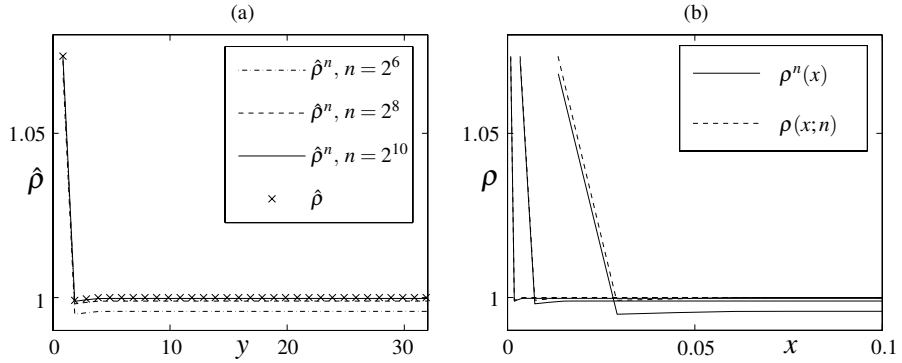

Fig. 12 Same setup as in Figure 9. Here, the density profiles are computed for $V = V_{\text{wall}}$ instead of V_2.

- $F_n(x^n)$ in (10) for the solution of (2);
- $F(\chi)$ in (10) for the solution of (47);
- $\tilde{F}$ in (11) for the equispaced particle configuration.

More specifically, we compute $F(\chi)$ and $\tilde{F}$ by the same approximation leading to (47), i.e.,

$$F(\chi) = -\sum_{i=1}^{J-1} V'(\chi(i)) - \frac{1}{2}V'(\chi(J)) + V(\chi(J)),$$
$$\tilde{F} = -\sum_{i=1}^{J-1} V'(i) - \frac{1}{2}V'(J) + V(J),$$

where $J = 1100$ in §5.2 and $J = 220$ in §5.3.

Table 2 shows the values of the force on the barrier and the predictions thereof as mentioned above. In §1.3 we discuss the implications of Table 2.

	n	V_2	V_{wall}
$F_n(x^n)$	2^3	2.750	1.059
	2^4	2.937	1.100
	2^5	3.071	1.122
	2^6	3.158	1.133
	2^7	3.213	1.139
	2^8	3.246	1.142
	2^9	3.265	1.143
	2^{10}	3.276	1.144
	2^{11}	3.282	1.145
	2^{12}	3.286	1.145
$F(\chi)$		3.289	1.145
$\tilde{F}$		2.404	0.913

Table 2 Values for the force which the particles exert on the barrier for two choices of the potential V and for various values of n. The formulae for the forces are specified in §5.4.

A Technical details of asymptotic matching

A.1 Asymptotic analysis using the bulk ansatz

We obtain asymptotic solutions for $x(i)$ in both the bulk and boundary layer regimes using the method of matched asymptotic expansions. The method that we use involves matching with an intermediate variable, and is analogous to the methods used in [20,43]. Whereas [20,43] concentrate on leading-order matching, we use the method to obtain higher order corrections. We begin by introducing a continuum bulk ansatz, $x(i;n) = \xi(in^{-1};n)$, which we assume to be valid when $i \gg 1$ and $n-i \gg 1$. At the same time, we introduce a discrete boundary layer ansatz, $x(i;n) = n^{-1}\chi(i;n)$, which we assume to be valid when $i \ll n$. Thus, both ansatzes are assumed to be valid asymptotic expansions when $1 \ll i \ll n$.

This means that we can introduce an arbitrary K with $1 \ll K \ll n$ and use the boundary layer ansatz for $x(i;n)$ when $i \leq K$ or $i \geq n-K$ and use the bulk ansatz for $x(i;n)$ when $K < i < n-K$. By the principles that underly the method of matched asymptotic expansions, the precise dependence of K on n should not matter; the behaviour of $\xi(s;n)$ as $s \to 0$ should match with the behaviour of $\chi(i;n)$ as $i \to \infty$ so as to yield consistent asymptotic expressions for $x(i)$ when $1 \ll i \ll n$ regardless of whether i is treated as being in the bulk regime or the boundary layer regime. We think of K as an arbitrary intermediate point where we connect the bulk ansatz with the boundary layer ansatz.

We make the following assumptions about the behaviour of $\xi(s;n)$ and $\chi(i;n)$:

(MinSpacing) There exists $M > 0$ such that $\chi(i+1) - \chi(i) \geq M$ whenever $i \ll n$, and $\xi'(s) \geq M$ whenever $s \gg n^{-1}$ and $1 - s \gg n^{-1}$.

(ξ-Smooth) $\xi \in C^\infty((\eta, 1-\eta))$ for any choice of η where $n^{-1} \ll \eta \ll 1$.

As previously, these statements must all hold true in the asymptotic limit as $n \to \infty$ where ξ and χ are replaced with

$$\xi(s) = \sum_{k=0}^{Q} n^{-b_k}\xi_k(s) + O\big(n^{-b_{Q+1}}\big), \quad \text{and} \quad \chi(i) = \sum_{j=0}^{P} n^{-\beta_j}\chi_j(i) + O\big(n^{-\beta_{P+1}}\big),$$

respectively for any choices of P and Q.

We note that **(MinSpacing)** implies that $\chi(i+1) - \chi(i) \geq M$ whenever $i \leq K$, and equally that

$$n\int_{\frac{i}{n}}^{\frac{i+1}{n}} \xi(s)\,\mathrm{d}s \geq M,$$

whenever $i \geq K$, regardless of the choice of K as long as $1 \ll K \ll n$. Hence, **(MinSpacing)** implies a minimum separation between particles that holds uniformly in n independently of the choice of 'cutoff' between the bulk region and the boundary layer region.

We also note that replacing χ and ξ with their leading order approximations in **(MinSpacing)** and considering the limits as $n \to \infty$, yields the result that $\chi_0(i+1) - \chi_0(i) \geq M$ and $\xi_0'(s) \geq M$ throughout.

Additionally, we observe that **(MinSpacing)** places growth restrictions on higher order corrections to χ and ξ'. Specifically, it means that $\chi_j(i+1)-\chi_j(i)$ cannot grow (negatively) at a rate greater than i^{β_j} as $i\to\infty$, and that $\xi_k'(s)$ cannot grow (negatively) at a rate greater than s^{-b_k} as $s\to 0$.

We further use the symmetry of the problem to assert that $\xi(1-s)=1-\xi(s)$ and that $x(n-i)=1-n^{-1}\chi(n-i;n)$ when $n-i=O(1)$. We also assume that the bulk ansatz and the discrete boundary layer ansatz are the only scalings that we need to consider for the method of matched asymptotic expansions. That is, we assume that there is no distinguished intermediate scaling between $i=\mathrm{ord}(n)$ and $i=\mathrm{ord}(1)$. A justification of this assumption can be obtained by using the methods described in §2.3.

Given that $V(x)=|x|^{-a}$, the force balance equation from (2) yields

$$an^{-a-1}\left(\sum_{k=1}^{i}\left[x(i)-x(i-k)\right]^{-a-1}-\sum_{k=1}^{n-i}\left[x(i+k)-x(i)\right]^{-a-1}\right)=0. \tag{54}$$

In the remainder of this section, we concentrate on analysing force balance in the bulk, where $i=\mathrm{ord}(n)$. As described above, we split the sums into regions where we apply the continuum ansatz for $x(i\pm k)$ and regions where we apply the discrete ansatz:

$$\underbrace{an^{-a-1}\sum_{k=0}^{K-1}\left(\left[\xi(in^{-1})-n^{-1}\chi(k)\right]^{-a-1}-\left[1-\xi(in^{-1})-n^{-1}\chi(k)\right]^{-a-1}\right)}_{S_0}$$
$$+an^{-a-1}\left(\sum_{k=1}^{i-K}\left[\xi(in^{-1})-\xi([i-k]n^{-1})\right]^{-a-1}-\sum_{k=1}^{n-K-i}\left[\xi([i+k]n^{-1})-\xi(in^{-1})\right]^{-a-1}\right)=0. \tag{55}$$

Since $K\ll n$, the sum marked S_0 in (55) is $o(n^{-a})$. From previously, we recognise that the leading order terms in the bulk force balance will be $\mathrm{ord}(n^{-1})$; hence, it will be possible to obtain expressions for $\xi(s)$ up to $o(n^{-(a-1)})$ while entirely neglecting any contributions from S_0. Higher order corrections to $\xi(s)$ may be obtained by expanding the summand of S_0 using Taylor series, and then exploiting the properties of $\chi(i)$. While it is possible to carry out these manipulations, we do not consider these high-order corrections in detail in this paper.

We can therefore follow the approach used previously and neglect S_0. This leads us to define the following force function, $F(s)$, noting that force balance in the bulk requires $F(s)=o(n^{-a})$ for all $s=\frac{i}{n}$ where $i=\mathrm{ord}(n)$ and $n-i=\mathrm{ord}(n)$:

$$F(s):=an^{-a-1}\left[\sum_{k=1}^{\lfloor sn-K\rfloor}\left[\xi(s)-\xi(s-kn^{-1})\right]^{-a-1}-\sum_{k=1}^{\lfloor n-K-sn\rfloor}\left[\xi(s+kn^{-1})-\xi(s)\right]^{-a-1}\right].$$

We now separate $F(s)$ into three parts as previously, introducing an arbitrary integer H where $n^{\frac{a}{a+1}}\ll H\ll n$:

$$F(s)=\underbrace{an^{-a-1}\sum_{k=1}^{H}\left(\left[\xi(s)-\xi(s-kn^{-1})\right]^{-a-1}-\left[\xi(s+kn^{-1})-\xi(s)\right]^{-a-1}\right)}_{=:S_1}$$
$$+\underbrace{an^{-a-1}\sum_{k=H+1}^{\lfloor sn\rfloor-K}\left[\xi(s)-\xi(s-kn^{-1})\right]^{-a-1}}_{=:S_2}$$
$$-\underbrace{an^{-a-1}\sum_{k=H+1}^{\lfloor n-sn\rfloor-K}\left[\xi(s+kn^{-1})-\xi(s)\right]^{-a-1}}_{=:S_3}. \tag{56}$$

We note that $H\gg n^{\frac{a}{a+1}}$ places restrictions on K, since we require $K\gg H$ in order for the sums S_2 and S_3 to contain large numbers of terms. This lower bound on K might suggest the presence of a distinguished scaling between $i=\mathrm{ord}(n)$ and $i=\mathrm{ord}(1)$, so that there is a continuum boundary layer problem to solve between the continuum bulk problem and the discrete boundary layer. We expect that the methods in §2.3

could be used to show that no such continuum boundary layer problem can exist and that hence the bulk ansatz is valid for all $i \gg 1$, but we do not pursue this analysis further.

We begin our analysis of (56) by considering S_2. Using the Euler–Maclaurin summation formula with an offset from the integers (see, for example, [39]), we find that

$$S_2 = an^{-a}\int_{Kn^{-1}}^{s-Hn^{-1}} \frac{\mathrm{d}u}{[\xi(s)-\xi(u)]^{a+1}} - an^{-a-1}\left(\frac{1}{2[\xi(s)-\xi(s-Hn^{-1})]^{a+1}} + \frac{B_1(\{sn\})}{[\xi(s)-\xi(Kn^{-1})]^{a+1}}\right) + a(a+1)n^{-a-1}\int_{Kn^{-1}}^{s-Hn^{-1}} \frac{B_1(\{sn+un\})\xi'(u)}{[\xi(s)-\xi(u)]^{a+2}}\,\mathrm{d}u, \quad (57)$$

where $B_1(\{\cdot\})$ is the 1-periodic extension of the first Bernoulli polynomial. Using **(MinSpacing)** we observe that $\xi(s)-\xi(s-Hn^{-1}) \geq MHn^{-1}$ and that $\xi(s)-\xi(Kn^{-1}) = \mathrm{ord}(1)$. Using Hölder's inequality to show that the integral remainder term is asymptotically no larger than the terms on the second line of (57), we therefore find that

$$S_2 = an^{-a}\int_{Kn^{-1}}^{s-Hn^{-1}} \frac{\mathrm{d}u}{[\xi(s)-\xi(u)]^{a+1}} + O(H^{-a-1}).$$

An identical argument applies to S_3. Using the fact that $H \gg n^{\frac{a}{1+a}}$ and $K \ll n$, we can combine the expansions of S_2 and S_3 to show that

$$S_2 + S_3 = an^{-a}\left[\int_0^{s-Hn^{-1}} \frac{\mathrm{d}u}{[\xi(s)-\xi(u)]^{a+1}} - \int_{s+Hn^{-1}}^1 \frac{\mathrm{d}u}{[\xi(u)-\xi(s)]^{a+1}}\right] + o(n^{-a}). \quad (58)$$

Now consider S_1. Using Taylor's theorem, **(ξ-Smooth)** implies that $\xi(s\pm kn^{-1})$ can be approximated by the series

$$\xi(s\pm kn^{-1}) \sim \xi(s) \pm \xi'(s)kn^{-1} + \tfrac{1}{2}\xi''(s)k^2n^{-2} + \ldots,$$

which is asymptotic for any $k \ll n$ and $s \gg n^{-1}$. Since $k \leq H \ll n$ in S_1 and $s = \mathrm{ord}(1)$ in our present analysis, we can apply this asymptotic expansion throughout. This yields

$$S_1 \sim a\sum_{k=1}^{H} k^{-a-1}\Big(\big[\xi'(s) - \tfrac{1}{2}kn^{-1}\xi''(s) + \tfrac{1}{6}k^2n^{-2}\xi'''(s) + \ldots\big]^{-a-1} - \big[\xi'(s) + \tfrac{1}{2}kn^{-1}\xi''(s) + \tfrac{1}{6}k^2n^{-2}\xi'''(s) + \ldots\big]^{-a-1}\Big). \quad (59)$$

Noting that $kn^{-1} \ll 1$, we can apply the binomial series and rearrange to obtain

$$S_1 \sim \sum_{k=1}^{H} k^{-a-1}\Big((-a)_2\xi''(s)\big[\xi'(s)\big]^{-a-2}kn^{-1} + \Big[\tfrac{1}{12}(-a)_2\big[\xi'(s)\big]^{-a-2}\xi''''(s) + \tfrac{1}{6}(-a)_3\big[\xi'(s)\big]^{-a-3}\xi''(s)\xi'''(s) + \tfrac{1}{24}(-a)_4\big[\xi'(s)\big]^{-a-4}\big[\xi''(s)\big]^3\Big]k^3n^{-3} + O(k^5n^{-5})\Big) \quad (60)$$

where $(\cdot)_r$ is the Pochhammer symbol, defined so that $(\alpha)_r := \alpha\cdot(\alpha-1)\cdots(\alpha-r+1)$. Since the summand in equation (60) is obtained by taking compositions of functions defined as formal series, we can use the properties of partial Bell polynomials (see, for example, [11,45]) to obtain a general expression for the terms in the summand of (60). Specifically, we find that

$$S_1 \sim \sum_{k=1}^{H}\sum_{p=0}^{\infty} \mathscr{B}_p[\xi](s)k^{-a+2p}n^{-(2p+1)}, \quad (61)$$

where

$$\mathscr{B}_p[\xi](s) := \left(\frac{2}{(2p+1)!}\sum_{q=1}^{2p+1} Y_{2p+1,q}\left[\frac{\xi''(s)}{2}, \frac{\xi'''(s)}{3}, \ldots, \frac{\xi^{(2p-q+3)}}{2p-q+3}\right](-a)_{q+1}\big[\xi'(s)\big]^{-a-1-q}\right), \quad (62)$$

and $Y_{p,q}(t_1,t_2,\ldots,t_{p-q+1})$ is a partial Bell polynomial. These polynomials are defined by the expression

$$Y_{p,q}(t_1,t_2,\ldots,t_{p-q+1}) = \sum \frac{p!}{r_1!r_2!\cdots r_{p-q+1}!}\left(\frac{t_1}{1!}\right)^{r_1}\left(\frac{t_2}{2!}\right)^{r_2}\cdots\left(\frac{t_{p-q+1}}{(p-q+1)!}\right)^{r_{p-q+1}},$$

where the sum is taken over all integer sequences $\{r_1, r_2, \ldots, r_{p-q+1}\}$ where

$$\sum_{k=1}^{p-q+1} k r_k = p, \quad \text{and} \quad \sum_{k=1}^{p-q+1} r_k = q.$$

As described in [11], partial Bell polynomials have the property that

$$\frac{1}{q!}\left[\sum_{j=1}^{\infty}\frac{x^j}{j!}t_j\right]^q = \sum_{p=q}^{\infty} Y_{p,q}(t_1,t_2,\ldots,t_{p-q+1})\frac{x^p}{p!}.$$

It is this property of partial Bell polynomials that makes it possible to obtain (62) from (59).

Since $kn^{-1} \ll 1$, it is possible to swap the order of summation in (61) while still retaining asymptoticity:

$$S_1 \sim \sum_{p=0}^{\infty}\mathscr{B}_p[\xi](s)\,n^{-(2p+1)}\sum_{k=1}^{H}k^{-a+2p}.$$

To evaluate the sum over k, we note from [20] that the asymptotic behaviour of the generalised harmonic numbers is given by

$$\sum_{k=1}^{H}k^{-r} = \begin{cases}\zeta(r)-\frac{1}{r-1}H^{-(r-1)}+O(H^{-r}), & r>1,\\ \log(H)+\gamma+O(H^{-1}), & r=1,\\ O(H^{1-r}), & r<1,\end{cases}$$

where γ is the Euler–Mascheroni constant. Then, from $n^{\frac{a}{a+1}} \ll H \ll n$ we obtain

$$\sum_{k=1}^{H}k^{-a+2p}n^{-(2p+1)} = \begin{cases}\zeta(a-2p)n^{-(2p+1)}-\frac{(Hn^{-1})^{-(a-2p-1)}}{a-2p-1}n^{-a}+o(n^{-a}), & 2p<a-1,\\ \big(\log(H)+\gamma\big)n^{-a}+o(n^{-a}) & 2p=a-1,\\ o(n^{-a}), & 2p>a-1,\end{cases}$$

and (61) yields

$$S_1 = \sum_{p=0}^{\lceil\frac{a-1}{2}\rceil-1}\left(\mathscr{B}_p[\xi](s)\left[\zeta(a-2p)n^{-(2p+1)}-\frac{(Hn^{-1})^{-(a-2p-1)}}{a-2p-1}n^{-a}\right]\right) + \mathbb{1}_{a\in 2\mathbb{N}+1}\mathscr{B}_{\frac{a-1}{2}}[\xi](s)\big[\log(H)+\gamma\big]n^{-a}+o(n^{-a}). \quad (63)$$

In order to simplify this expression into a form where it can be combined with (58), it is useful to introduce finite part integration. Following [28,32], we define the one-sided finite part integral for functions that are well-behaved apart from a possible singularity at zero, and which satisfy

$$\psi(u) = \sum_{j=0}^{\Upsilon-1}c_j u^{-a_j}+c_\Upsilon u^{-1}+O(u^{-1+\delta}), \quad \text{as } u\to 0,$$

where $a_0 > a_1 > \ldots > a_{\Upsilon-1} > 1$ and $\delta > 0$. In this case, we define

$$\fint_0^y \psi(u)\,\mathrm{d}u := \lim_{\eta\to 0}\left[\int_\eta^y \psi(u)\,\mathrm{d}u - \sum_{j=0}^{\Upsilon-1}\frac{c_j\eta^{-(a_j-1)}}{a_j-1}-c_\Upsilon\log\frac{1}{\eta}\right]. \quad (64)$$

From (61), we note that

$$a\big[\xi(s)-\xi(s-u)\big]^{-a-1}-a\big[\xi(s+u)-\xi(s)\big]^{-a-1} = \sum_{p=0}^{\lfloor\frac{a-1}{2}\rfloor}\mathscr{B}_p[\xi](s)u^{-(a-2p)}+O\left(u^{1+2\lfloor\frac{a}{2}\rfloor-a}\right).$$

Then, using (64), we obtain

$$\fint_0^y a\big[\xi(s)-\xi(s-u)\big]^{-a-1}-a\big[\xi(s+u)-\xi(s)\big]^{-a-1}\,\mathrm{d}u \\ =-\sum_{p=0}^{\lceil\frac{a-1}{2}\rceil-1}\mathscr{B}_p[\xi](s)\frac{y^{-(a-2p-1)}}{a-2p-1}+\mathbb{1}_{a\in 2\mathbb{N}+1}\mathscr{B}_{\frac{a-1}{2}}[\xi](s)\log(y)+o(1)$$

as $y\to 0$. Hence, (63) becomes

$$S_1=\sum_{p=0}^{\lceil\frac{a-1}{2}\rceil-1}\mathscr{B}_p[\xi](s)\zeta(a-2p)n^{-(2p+1)} \\ +an^{-a}\fint_0^{Hn^{-1}}\big[\xi(s)-\xi(s-u)\big]^{-a-1}-\big[\xi(s+u)-\xi(s)\big]^{-a-1}\,\mathrm{d}u \\ +\mathbb{1}_{a\in 2\mathbb{N}+1}\mathscr{B}_{\frac{a-1}{2}}[\xi](s)\big[\log(n)+\gamma\big]n^{-a}+o(n^{-a}).$$

Combining with (58), we therefore find that

$$F(s)=\sum_{p=0}^{\lceil\frac{a-1}{2}\rceil-1}\mathscr{B}_p[\xi](s)\zeta(a-2p)\,n^{-(2p+1)} \\ +\left(\mathbb{1}_{a\in 2\mathbb{N}+1}\mathscr{B}_{\frac{a-1}{2}}[\xi](s)\big[\log(n)+\gamma\big]+a\fint_0^1\frac{\operatorname{sgn}(s-u)}{|\xi(s)-\xi(u)|^{a+1}}\,\mathrm{d}u\right)n^{-a}+o\big(n^{-a}\big). \quad (65)$$

In the more general case where V satisfies (30), we find that much of the argument outlined in this section still holds. Since it is possible to approximate $V'(x)$ by $-ax^{-a-1}$ for large x, we find that S_2+S_3 will still be given by (58). The most significant changes required to generalise our argument involve the manipulation of S_1. Repeated use of Taylor series (analogous to the manipulations of V in §2.2) are needed to obtain a new definition for $\mathscr{B}_p$ for a general V; specifically, we find that $(-a)_{q+1}[\xi'(s)]^{-a-1-q}$ in (62) should be replaced with $k^{a+1+q}V^{(q+1)}[\xi'(s)k]$.

While it is true that

$$k^{a+1+q}V^{(q+1)}[\xi'(s)k]\to(-a)_{q+1}[\xi'(s)]^{-a-1-q}\quad\text{as } k\to\infty,$$

the fact that the modified definition of $\mathscr{B}_p$ involves k creates complications for the manipulation of sums involving k through the rest of the argument. Ultimately, we find that the asymptotic properties of these sums mean that the approach outlined above remains valid, and that the analogous equation to (65) is

$$F(s)=\sum_{p=0}^{\lceil\frac{a-1}{2}\rceil-1}\tilde{\mathscr{B}}_p[\xi](s)n^{-(2p+1)} \\ +\left(\mathbb{1}_{a\in 2\mathbb{N}+1}\left[\tilde{\mathscr{B}}_{\frac{a-1}{2}}[\xi](s)\log(n)+\mathscr{G}[\xi]\right]+a\fint_0^1\frac{\operatorname{sgn}(s-u)}{|\xi(s)-\xi(u)|^{a+1}}\,\mathrm{d}u\right)n^{-a}+o\big(n^{-a}\big),$$

where $\tilde{\mathscr{B}}_p$, $\tilde{\mathscr{B}}_{\frac{a-1}{2}}$, and $\mathscr{G}$ depend on V. Note that the terms which gave rise to the zeta function and Euler–Mascheroni constant in (65) are replaced with new formulations that depend on V and ξ', but the overall structure of the total force from (65) remains the same. We find that

$$\tilde{\mathscr{B}}_0[\xi](s)=\xi''(s)\sum_{k=1}^{\infty}V''[\xi'(s)k]k^2, \quad (66)$$

and that $\tilde{\mathscr{B}}_p[\xi]$, $\tilde{\mathscr{B}}_{\frac{a-1}{2}}[\xi]$ and $\mathscr{G}[\xi]$ all evaluate to the zero function when ξ is affine. These observations enable us to extend the results of the following section to more general potentials V that satisfy (30).

A.2 Solving for higher order corrections in the bulk

We now return to the case where $V(x) = |x|^{-a}$ and we seek an asymptotic expansion of $\xi(s)$ that will enable (55) to be satisfied for integers i where $i \gg K$ and $n-i \gg K$. If we restrict our analysis to corrections up to ord $\left[n^{-(a-1)}\right]$, we find that this is equivalent to seeking $\xi(s)$ so that $F(s) = o(n^{-a})$, and hence we can make immediate use of (65). Thus, we begin by expanding $\xi(s)$ as an asymptotic series as follows:

$$\xi(s) = \xi_0(s) + \sum_{k=1}^{\bar{Q}} n^{-b_k}\xi_k(s) + n^{-(a-1)}\tilde{\xi}(s) + o(n^{-(a-1)}), \qquad 0 < b_1 < \ldots < b_{\bar{Q}} < a-1; \tag{67}$$

where $\bar{Q}$ may perhaps be infinite or zero.

On substituting (67) into (65), we find that the largest nontrivial terms are recovered at $O(n^{-1})$. These yield the result that $\zeta(a)\mathscr{B}_0[\xi_0](s) = 0$. Using the definition of $\mathscr{B}_p[\xi]$ in (62), this becomes

$$\zeta(a)(-a)_2\xi_0''(s)\left[\xi_0'(s)\right]^{-a-2} = 0,$$

and hence $\xi_0(s)$ is affine. More specifically, we can use the leading order boundary conditions from (15) to conclude that $\xi_0'(s) = 1$ and $\xi_0(s) = s$.

In order to characterise the next nontrivial term in the expansion of $F(s)$, we assume for the moment that $b_1 < a-1$ to avoid dealing with the singular integral term at $O(n^{-a})$. Since $\xi_0'(s)$ is constant and nonzero, it follows from (62) that $\mathscr{B}_p[\xi_0] \equiv 0$ for all p. Hence, the next nontrivial terms in the expansion of (65) appear at $O(n^{-1-b_1})$, where we find that

$$\zeta(a)(-a)_2\xi_1''(s) = 0.$$

Again, we conclude that $\xi_1(s)$ is affine and we find that $\mathscr{B}_p[\xi_0 + n^{-b_1}\xi_1] \equiv 0$ for all p. We cannot apply boundary conditions to $\xi_1(s)$ at this stage, since the boundary conditions on ξ_1 will depend on the matching between the bulk solution and the boundary layer solution. However, we can use the symmetry of the force balance problem to conclude that $\xi_1(s) = -\xi_1(1-s)$ and hence

$$\xi_1(s) = (s - \tfrac{1}{2})p_1$$

where $p_1 = \xi_1'(s)$ is a constant to be determined from matching with the boundary layer.

As long as $b_k < a-1$ we can apply the same argument to show that ξ_k is affine. We will use this freedom in the choice of b_k later on to match with the boundary layer. For now, we rewrite the expansion of ξ in (67) as

$$\xi(s) = s + \bar{p}(n)(s - \tfrac{1}{2}) + n^{-(a-1)}\tilde{\xi}(s) + o(n^{-(a-1)})$$

where $\bar{p} := p_1 n^{-b_1} + p_2 n^{-b_2} + \ldots$, so that $\bar{p} \ll 1$. This yields

$$n^{-a}\left[\zeta(a)(-a)_2\tilde{\xi}''(s) + a\fint_0^1 \frac{\operatorname{sgn}(s-u)}{|s-u|^{a+1}}\,\mathrm{d}u\right] = o(n^{-a}).$$

Next we solve for $\tilde{\xi}$. Since

$$a\fint_0^1 \frac{\operatorname{sgn}(s-u)}{|s-u|^{a+1}}\,\mathrm{d}u = (1-s)^{-a} - s^{-a},$$

we have that

$$\tilde{\xi}''(s) = \frac{s^{-a} - (1-s)^{-a}}{\zeta(a)(-a)_2}.$$

By using again the symmetry of the force balance (i.e. $\tilde{\xi}(s) = -\tilde{\xi}(1-s)$), we obtain

$$\tilde{\xi}(s) = \begin{cases} \dfrac{s^{-(a-2)} - (1-s)^{-(a-2)}}{\zeta(a)(-a+2)_4} + (s-\tfrac{1}{2})\tilde{p}, & a \neq 2 \\ \dfrac{\log(1-s) - \log(s)}{\pi^2} + (s-\tfrac{1}{2})\tilde{p}, & a = 2. \end{cases} \tag{68}$$

where $\tilde{p}$ is a constant to be determined from matching with the boundary layer.

In the more general case where V satisfies (30), we still find that $\xi_k(s) = p_k(s-\frac{1}{2})$ whenever $b_k < a-1$ as a consequence of the fact that $\bar{\mathscr{B}}_p[\xi] \equiv 0$ when ξ is affine. We can also evaluate $\bar{\xi}$ by using the definition of $\bar{\mathscr{B}}_0$ given in (66). This yields

$$\bar{\xi}(s) = \begin{cases} \dfrac{s^{-(a-2)} - (1-s)^{-(a-2)}}{Z(V)(-a+2)_2} + (s-\frac{1}{2})\tilde{p}, & a \neq 2 \\ \dfrac{\log(1-s) - \log(s)}{Z(V)} + (s-\frac{1}{2})\tilde{p}, & a = 2. \end{cases} \tag{69}$$

where

$$Z(V) := \sum_{k=1}^{\infty} V''(k)k^2.$$

A.3 Asymptotic analysis in the boundary layer

We now return to assuming $V(x) = |x|^{-a}$ and seek solutions for $\chi_j(i)$ by considering the case where $i = \mathrm{ord}(1)$ in (54). We recall that we introduced K at the beginning of §A.1 so that $1 \ll K \ll n$, and hence K is in the intermediate region where both the boundary layer ansatz and the bulk ansatz can be used.

Assuming $i = \mathrm{ord}(1)$, we split the sums in (54) to obtain

$$\underbrace{a\sum_{\substack{k=0\\k\neq i}}^{K} \frac{\mathrm{sgn}(i-k)}{|\chi(i)-\chi(k)|^{a+1}}}_{S_4} \underbrace{-an^{-a-1}\sum_{k=K+1}^{n-K-1}\left[\xi(kn^{-1}) - n^{-1}\chi(i)\right]^{-a-1}}_{S_5}$$
$$\underbrace{-an^{-a-1}\sum_{k=0}^{K}\left[1 - n^{-1}\chi(k) - n^{-1}\chi(i)\right]^{-a-1}}_{S_6} = 0. \tag{70}$$

Since all the terms in the summand of S_6 are $O(1)$, we find that $S_6 = O(Kn^{-a-1}) = o(n^{-a})$. Moreover, using **(MinSpacing)** we obtain that

$$S_5 \lesssim n^{-a-1}\sum_{k=K+1}^{n-K-1}\left[Mkn^{-1}\right]^{-a-1} \lesssim \sum_{k=K}^{\infty} k^{-a-1} = O(K^{-a}),$$

and hence (70) becomes

$$a\sum_{\substack{k=0\\k\neq i}}^{K} \mathrm{sgn}(i-k)|\chi(i)-\chi(k)|^{-a-1} = O\big(K^{-a}\big). \tag{71}$$

Following the methods described in §2.4, it follows that the leading order solution in the boundary layer is a solution to the infinite system of algebraic equations

$$a\sum_{\substack{k=0\\k\neq i}}^{\infty} \mathrm{sgn}(i-k)|\chi_0(i)-\chi_0(k)|^{-a-1} = 0, \quad i = 1, 2, \ldots$$

subject to the matching condition $\chi_0(i) - \chi_0(i-1) \to 1$ as $i \to \infty$.

To obtain higher order corrections, we begin by assuming an asymptotic power series expansion for $\chi(i)$. As in §A.2, we will seek solutions up to ord$[n^{-(a-1)}]$ and thus it is convenient to introduce a power series of the form

$$\chi(i) = \chi_0(i) + \sum_{j=1}^{\bar{P}} n^{-\beta_j}\chi_j(i) + n^{-(a-1)}\tilde{\chi}(i) + o[n^{-(a-1)}], \qquad 0 < \beta_1 < \ldots < \beta_{\bar{P}} < a-1; \tag{72}$$

where $\bar{P}$ may be zero or infinite.

As we discuss in §A.4, asymptotic matching implies that $\chi_j(i)-\chi_j(i-1)$ must have a finite limit as $i\to\infty$ for any $\beta_j<a-1$, and an identical result holds for $\tilde{\chi}(i)-\tilde{\chi}(i-1)$. The fact that these limits are finite enables us to make significant simplifications after we substitute (72) into (71). Applying the multinomial expansion, we see that this yields

$$\begin{aligned}a\sum_{\substack{k=0\\k\neq i}}^{K}\operatorname{sgn}(i-k)|\chi(i)-\chi(k)|^{-a-1}\sim{}& a\sum_{\substack{k=0\\k\neq i}}^{K}\operatorname{sgn}(i-k)|\chi_0(i)-\chi_0(k)|^{-a-1}\\&-n^{-\beta_1}a(a+1)\sum_{\substack{k=0\\k\neq i}}^{K}|\chi_0(i)-\chi_0(k)|^{-a-2}[\chi_1(i)-\chi_1(k)]\\&-n^{-\beta_2}a(a+1)\sum_{\substack{k=0\\k\neq i}}^{K}|\chi_0(i)-\chi_0(k)|^{-a-2}[\chi_2(i)-\chi_2(k)]\\&+\frac{n^{-2\beta_1}}{2}a(a+1)(a+2)\sum_{\substack{k=0\\k\neq i}}^{K}|\chi_0(i)-\chi_0(k)|^{-a-3}[\chi_1(i)-\chi_1(k)]^2+\ldots=O(K^{-a}).\end{aligned}\tag{73}$$

Since $\chi_j(i)-\chi_j(k)\sim C_j(i-k)$ for some constant C_j as $k\to\infty$, it follows that

$$\sum_{k=K+1}^{\infty}\operatorname{sgn}(i-k)|\chi_0(i)-\chi_0(k)|^{-a-1}=O(K^{-a}),$$
$$\sum_{k=K+1}^{\infty}|\chi_0(i)-\chi_0(k)|^{-a-2}[\chi_1(i)-\chi_1(k)]=O(K^{-a}),$$

and so on. This enables us to extend the sums in (73) to infinity without introducing significant errors. Choosing K so that $n^{1-\frac{1}{a}}\ll K\ll n$, we therefore find that (71) becomes

$$\begin{aligned}a\sum_{\substack{k=0\\k\neq i}}^{\infty}\operatorname{sgn}(i-k)|\chi_0(i)-\chi_0(k)|^{-a-1}&\\-n^{-\beta_1}a(a+1)\sum_{\substack{k=0\\k\neq i}}^{\infty}|\chi_0(i)-\chi_0(k)|^{-a-2}[\chi_1(i)-\chi_1(k)]+\ldots=o[n^{-(a-1)}].&\end{aligned}$$

Collecting $\operatorname{ord}(n^{-\beta_1})$ terms, we obtain the following infinite homogeneous linear system for system for $\chi_1(i)$:

$$-a(a+1)\sum_{\substack{k=0\\k\neq i}}^{\infty}|\chi_0(i)-\chi_0(k)|^{-a-2}[\chi_1(i)-\chi_1(k)]=0,\quad i=1,2,\ldots,\tag{74}$$

where $\chi_1(0)=0$ due to the fact that $x(0)=0$. This system must be solved subject to some matching condition that relates the behaviour of $\chi_1(i)$ as $i\to\infty$ to the behaviour of the bulk solution as $s\to 0$. Since $|\chi_0(i)-\chi_0(k)|^{-a-2}=O(k^{-a-2})$ as $k\to\infty$, we observe that the sums in (74) are absolutely convergent when $\chi_1(k)=O(k^{a+1-\delta})$ for some $\delta>0$. Since asymptotic matching gives $\chi_j(k)=O(k)$ as $k\to\infty$ for all $\beta_j<a-1$, it follows that the sums in (74) are absolutely convergent for any i.

In §A.4, we show that asymptotic matching can be used to determine the exponents β_j and b_k. As we will see, this analysis relies on the claim that if (74) is solved subject to the particular matching condition $\chi_1(i)-\chi_1(i-1)\to 0$, then the only possible solution is the trivial solution, $\chi_1(i)\equiv 0$. To prove this claim, we observe that (74) is a linear equation of the type $\mathscr{A}\chi_1=0$, where we interpret $(\chi_1(i))_{i=1}^{\infty}$ as a sequence and $\mathscr{A}$ as an infinite matrix A with entries

$$A_{ij}:=\left\{\begin{array}{ll}-|\chi_0(i)-\chi_0(j)|^{-a-2}, & \text{if } i\neq j\\ \displaystyle\sum_{\substack{k=0\\k\neq i}}^{\infty}|\chi_0(i)-\chi_0(k)|^{-a-2}, & \text{if } i=j\end{array}\right\},\qquad \text{for } i,j\geq 1.$$

Since A is strictly diagonally dominant and symmetric, $\zeta\mapsto\zeta^T\mathscr{A}\zeta$ is a positive, strictly convex function on the space of sequences satisfying the matching condition $\zeta(i)-\zeta(i-1)\to 0$, and is thus uniquely globally

minimised when $\zeta = 0$. Since any χ_1 satisfying $\chi_1(k) = O(k)$ and $\mathscr{A}\chi_1 = 0$ also satisfies $\chi_1^T \mathscr{A}\chi_1 = 0$, it follows that $\chi_1 = 0$, which proves the claim.

A corollary of this claim is that any solution obtained to (74) subject to the matching condition $\chi_1(i) - \chi_1(i-1) \to p$ is unique, since otherwise the difference between two such solutions would be a nonzero solution to (74) that satisfies $\chi_1(i) - \chi_1(i-1) \to 0$.

From the form of (73), we observe that each higher correction χ_j will satisfy an infinite linear system of the form

$$-a(a+1) \sum_{\substack{k=0 \\ k \neq i}}^{\infty} |\chi_0(i) - \chi_0(k)|^{-a-2} \left[\chi_j(i) - \chi_j(k)\right] = g_j(i), \quad i = 1, 2, \ldots, \tag{75}$$

where $g_j(i)$ is obtained from the $\mathrm{ord}(n^{-\beta_j})$ terms in the multinomial expansion of $|\chi(i) - \chi(k)|^{-a-1}$, which in turn only depend on $\chi_0, \ldots, \chi_{j-1}$. Once an appropriate matching condition is specified in the form $\chi_j(i) - \chi_j(i-1) \to q_j$ for some constant q_j, we find that there will be a unique solution for χ_j. Similarly, $\tilde{\chi}$ will satisfy a linear system of the form given in (75), and the identical style of matching condition will be required.

We note that $g_j(i)$ will only be nonzero if β_j can be expressed as the sum of β_J values (possibly including repetitions) where $J < j$. For example, g_2 will only be nonzero if β_2 is a multiple of β_1. Since the linear system for χ_j above is identical to the linear system for χ_1, we see that $\chi_j(i) - \chi_j(i-1) \not\to 0$ as $i \to \infty$ is necessary for χ_j to have a nontrivial solution unless g_j is nonzero. This is an important observation for performing the matched asymptotic analysis in §A.4.

In the more general case where V satisfies (30), we find with very minor modifications of the analysis above that each χ_j satisfies the infinite linear system

$$-\sum_{\substack{k=0 \\ k \neq i}}^{\infty} V''\left[\chi_0(i) - \chi_0(k)\right] \left[\chi_j(i) - \chi_j(k)\right] = g_j(i), \quad i = 1, 2, \ldots,$$

where the functions $g_j(i)$ are obtained from Taylor series expansions of $V'(\chi(i) - \chi(k))$.

A.4 Matching between the bulk and the boundary layer

We established in §A.2 that ξ can be expanded as an asymptotic series of the form (67) where $\xi_k(s) = (s - \frac{1}{2})p_k$ and $\tilde{\xi}$ is given in (68). Additionally, we established in §A.3 that χ can be expanded as an asymptotic series of the form (72), where χ_j for $j > 0$ and $\tilde{\chi}$ are all solutions to infinite linear systems subject to a condition of the form $\chi_j(i) - \chi_j(i-1) \to q_j$ (and similarly for $\tilde{\chi}$). However, we have not yet characterised the exponents b_k and β_j in the power series (67) and (72), neither have we determined the constants p_k, $\tilde{p}$, q_j and $\tilde{q}$. We achieve this by using the method of matched asymptotic expansions.

We perform our asymptotic matching by introducing an intermediate matching variable, R, where R is an integer with $1 \ll R \ll n$. We assert that this R lies in the 'overlap region', so that both the bulk ansatz and the boundary layer ansatz yield asymptotic series solutions for $x(R;n)$ when $1 \ll R \ll n$. This involves making some assumptions about the asymptoticity of the bulk and boundary layer solutions outside the domains in which they are naturally defined. For example, we recall that we assumed that $i = \mathrm{ord}(n)$ in order to obtain the bulk equations described in §A.1. We now assert that the bulk series solution obtained in §A.2 remains valid whenever $i \gg 1$. That is, we assert that $\xi_0(Rn^{-1}) \gg n^{-b_k}\xi_k(Rn^{-1})$ for any $k > 0$ as long as $R \gg 1$. Despite the fact that $\tilde{\xi}(s)$ becomes unbounded as $s \to 0$, we observe that this assumption is consistent with comparing $\xi_0(s) = s$ with the solution for $\tilde{\xi}$ given in (68).

The matching variable, R, is distinct from the cut-off, K, used in several of the sums. We introduce the matching variable in order to analyse the relationship between the solution of the discrete boundary layer problem and the solution of the continuum bulk problem, whereas we introduce K in order to account for the 'bulk' and 'boundary layer' contributions to the force on any individual particle.

Asymptotic matching requires that $\xi(Rn^{-1})$ and $n^{-1}\chi(R)$ should be asymptotically equivalent throughout the overlap region. That is, we require that

$$\xi_0(Rn^{-1}) + n^{-b_1}\xi_1(Rn^{-1}) + \ldots \sim n^{-1}\chi_0(R) + n^{-\beta_1-1}\chi_1(R) + \ldots, \tag{76}$$

for all choices of R with $1 \ll R \ll n$. Each term obtained from expanding $\xi(Rn^{-1})$ under the assumption that Rn^{-1} is small should match with an equivalent term obtained from expanding $n^{-1}\chi(R)$ under the assumption that R is large. In the case where logarithmic terms and related complications are absent, this can be conveniently expressed using a matching table, in which the rows represent asymptotic expansions of $n^{-b_k}\xi_k(Rn^{-1})$

for small Rn^{-1} and the columns represent expansions of $n^{-\beta_j-1}\chi_j(R)$ for large R. Every row and column of the matching table should be a valid asymptotic series when $1 \ll R \ll n$, and every term in the interior of the table should be asymptotically larger than the terms below and to the right.

In order to construct a plausible matching table, we begin by exploiting the information that we already have about the functions ξ_k and $\tilde{\xi}$. Specifically, we observe from our analysis in §A.2 that

$$n^{-b_k}\xi_k(Rn^{-1}) = -\tfrac{p_k}{2}n^{-b_k} + p_k Rn^{-b_k-1}, \text{ wherever } b_k < a-1, \tag{77}$$

while the further assumption that $a \neq 2$ yields

$$\begin{aligned} n^{-(a-1)}\tilde{\xi}(Rn^{-1}) = {} & \frac{1}{\zeta(a)(-a+2)_4}R^{-(a-2)}n^{-1} \\ & - \left(\frac{1}{\zeta(a)(-a+2)_4} + \frac{\tilde{p}}{2}\right)n^{-(a-1)} + \left(\frac{1}{\zeta(a)(-a+1)_3} + \tilde{p}\right)Rn^{-a} + O(R^2 n^{-(a+1)}). \end{aligned} \tag{78}$$

Based on these results, we construct the following 'matching table' where each row and column can be read as an equation:

$$\begin{array}{ccccccccccc}
x(i;n) & \sim & n^{-1}\chi_0(R) & + & n^{-\beta_1-1}\chi_1(R) & + & \cdots & + & n^{-a}\tilde{\chi}(R) & + & \cdots \\
\wr & & \wr & & \wr & & & & \wr & & \\
\xi_0(Rn^{-1}) & = & Rn^{-1} & & & & & & & & \\
+ & & + & & & & & & & & \\
n^{-b_1}\xi_1(Rn^{-1}) & = & -\frac{p_1}{2}n^{-b_1} & + & p_1 Rn^{-b_1-1} & & & & & & \\
+ & & & & + & & & & & & \\
n^{-b_2}\xi_2(Rn^{-1}) & = & & & -\frac{p_2}{2}n^{-b_2} & + & \cdots & & & & \\
+ & & + & & + & & & & & & \\
\vdots & & \vdots & & \vdots & & \ddots & & & & \\
\vdots & & \vdots & & \vdots & & & & & & \\
+ & & + & & & & & & & & \\
n^{-(a-1)}\tilde{\xi}(Rn^{-1}) & \sim & \tilde{\kappa}_4 R^{-(a-2)}n^{-1} & & & + & \cdots & + & (\tilde{\kappa}_3+\tilde{p})Rn^{-a} & + & \cdots \\
+ & & + & & + & & & & + & & \\
\vdots & & \vdots & & \vdots & & \ddots & & \vdots & & \ddots \\
\vdots & & \vdots & & \vdots & & & & \vdots & &
\end{array}$$

where $\tilde{\kappa}_r := \frac{1}{\zeta(a)(-a+2)_r}$.

The matching table illustrates the fact that each term in the expansions of $n^{-b_k}\xi_k(Rn^{-1})$ given in (77) and (78) must correspond to an equivalent term in the asymptotic expansion of one of the functions $n^{-\beta_j-1}\chi_j(R)$. While the entries in the matching table above are based on the expansions of ξ_k, the columns must also be valid series. This places significant restrictions on the choices of b_k and β_j; for example, inspection of the $n^{-1}\chi_0(R)$ column of the matching table strongly suggests that $b_1 = 1$.

More rigorously, we can determine the values of b_k and β_j without appealing directly to the matching table. Since $n^{-b_k}\xi_k(Rn^{-1})$ is given by (77) when $b_k < a-1$, we find that the only terms on the left hand side of (76) that take the form $c_{\tau\upsilon}n^{-\tau}R^{\upsilon}$ for nonzero $c_\tau\upsilon$ are terms where $\upsilon = 1$ or $\upsilon = 0$ or $\upsilon \leq \tau - a + 1$. This third possibility is associated with the case where $b_k \geq a-1$ and hence $n^{-b_k}\xi_k(Rn^{-1})$ may not be linear.

Since every term on the right hand side of (76) must balance with an identical term on the left hand side of (76), this implies that

$$\chi_j(R) = \begin{cases} q_j R + \hat{q}_j + O(R^{\beta_j-(a-2)}), & \beta_j < a-2; \\ q_j R + O(R^{\beta_j-(a-2)}), & a-2 \leq \beta_j < a-1; \end{cases} \tag{79}$$

where q_j and $\hat{q}_j$ are constants. In order to match between equivalent terms on either side of (76), we find that the values of the constants q_j and $\hat{q}_j$ will be associated with values of p_k. Since (79) is concerned with the behaviour of $\chi_j(R)$ when R is large, we note that differencing (79) also provides justification of the fact that $\chi_j(i) - \chi_j(i-1)$ has a finite limit as $i \to \infty$ wherever $\beta_j < a-1$. More rigorously, this result could be established by exploiting the assumed differentiability of ξ and considering asymptotic matching between $\xi'(Rn^{-1})$ and $\chi(R) - \chi(R-1)$.

Now, let us assume that there exists some b_k in the range $0 < b_k < a-1$. By matching terms on either side of (76) and using (77), we find that both b_k and $b_k - 1$ must be values taken by exponents β_j. Since the smallest β_j is $\beta_0 = 0$, it follows that $b_k \geq 1$. If $a < 2$, this leads to a contradiction with the requirement that $b_k < a-1$, and we would therefore conclude that there are no exponents b_k in the range $0 < b_k < a-1$.

The case where $a > 2$ is a little more complicated. In order to analyse this problem, we recall from §A.3 that if $0 < \beta_j < a-1$, then $q_j = 0$ implies either that $\chi_j(i)$ has only the trivial solution $\chi_j(i) \equiv 0$, or that β_j can be expressed as the sum of other β_J values (allowing possible repetitions), where all of these other β_J are associated with nontrivial solutions for $\chi_J(i)$. Using this result, we show that the only possible b_k with $0 < b_k < a-1$ are the integers.

For the purposes of contradiction, assume that $a > 2$ and that there exists some smallest noninteger θ in the range $0 < \theta < a-1$ so that $b_k = \theta$ is associated with a nontrivial solution for ξ_k. As noted above, this implies that both $\theta - 1$ and θ must be values taken by the exponents β_j. Now, consider the function $\chi_j(i)$ associated with $\beta_j = \theta - 1$. Since this has a nontrivial solution, it follows that either $q_j \neq 0$ or that $\theta - 1$ can be expressed as the sum of β_J values associated with nontrivial solutions for χ_J. However, $q_j \neq 0$ would imply that the matching table contains a term of the form $q_j R n^{-\theta}$, which must correspond to $\theta - 1$ being a value taken by one of the b_k; this would be a contradiction with the assumption that θ is the smallest noninteger value of b_k. Similarly, if $\theta - 1$ can be expressed as a sum of β_J values, at least one of these must be noninteger, which would also lead to a contradictory noninteger value of b_k less than θ.

For $a \neq 2$, we therefore find that the solution in the bulk region takes the form

$$\xi(s) = s + \sum_{k=1}^{\lceil a-2 \rceil} p_k (s - \tfrac{1}{2}) n^{-k} + n^{-(a-1)} \tilde{\xi}(s) + o\big(n^{-(a-1)}\big),$$

where $\tilde{\xi}(s)$ is given in (68). Using either intermediate matching (as described above) or Van Dyke's matching criterion, we can use this expression to find the asymptotic behaviour of the functions $\chi_j(i)$ as $i \to \infty$. It follows that the solution in the boundary layer region takes the form

$$\chi(i) = \chi_0(i) + \sum_{j=1}^{\lceil a-2 \rceil} \chi_j(i) n^{-j} + n^{-(a-1)} \tilde{\chi}(i) + o\big(n^{-(a-1)}\big). \tag{80}$$

Moreover, we can use the matching table to define the asymptotic behaviour of $\chi_j(i)$ as $i \to \infty$ in terms of the constants p_k and $\tilde{p}$ from the solution in the bulk region. Specifically, we find that the asymptotic behaviour of $\chi_j(i)$ for large i and $a > 2$ is given by

$$\chi_j(i) = \begin{cases} i - \frac{p_1}{2} + \frac{1}{\zeta(a)(-a+2)_4} i^{-(a-2)} + o(i^{-(a-2)}), & j = 0; \\ p_j i - \frac{p_{j+1}}{2} + O\big(i^{-(a-2-j)}\big), & 0 < j < a-2; \\ p_j i - \left(\frac{1}{\zeta(a)(-a+2)_4} + \frac{\tilde{p}}{2} \right) + o(1), & j = a-2; \\ p_j i + O\big(i^{-(a-2-j)}\big), & a-2 < j < a-1, \end{cases} \tag{81}$$

The behaviour of $\tilde{\chi}(i)$ for large i is given by

$$\tilde{\chi}(i) = \left(\frac{1}{\zeta(a)(-a+1)_3} + \tilde{p} \right) i + o(i).$$

These expressions enable us to define the constants p_j based on the solutions obtained for $\chi_j(i)$. For $1 \leq j < a-1$, we see that

$$p_j = 2 \lim_{i \to \infty} \left[p_{j-1} i - \chi_{j-1}(i) \right],$$

where we take $p_0 = 1$. If a is an integer, we also find that

$$\tilde{p} = 2 \lim_{i \to \infty} \left[p_{a-1} i - \chi_{a-1}(i) \right] - \frac{2}{\zeta(a)(-a+2)_4}.$$

If a is not an integer, we require that $\tilde{p} = -\frac{2}{\zeta(a)(-a+2)_4}$. If this were not the case, (78) would yield an $\operatorname{ord}[R^0 n^{-(a-1)}]$ term on the left hand side of (76) that could not be balanced by any equivalent term on the right hand side of (76) without contradicting the result that χ has an expansion of the form given in (80).

In the case where $a < 2$, we recall that $\xi(s)$ must take the form

$$\xi(s) = s + n^{-(a-1)} \left[\frac{s^{-(a-2)} - (1-s)^{-(a-2)}}{\zeta(a)(-a+2)_4} + (s - \tfrac{1}{2}) \tilde{p} \right] + o\big(n^{-(a-1)}\big).$$

By the same argument as above for noninteger a when $a > 2$, we find that $\tilde{p} = -\frac{2}{\zeta(a)(-a+2)_4}$ also when $a < 2$. Hence, we find from (80) that $\chi(i) = \chi_0(i) + n^{-(a-1)}\tilde{\chi}(i)$ and that the asymptotic behaviours of these functions are given by

$$\chi_0(i) \sim i + \tfrac{1}{\zeta(a)(-a+2)_4} i^{-(a-2)} + o(i^{-(a-2)}), \tag{82}$$

and

$$\tilde{\chi}(i) = \tfrac{-a}{\zeta(a)(-a+2)_4} i + o(i).$$

In the case where $a = 2$, the logarithm in (68) requires careful handling, and we find that some additional terms that are logarithmically large in n need to be introduced. This makes it more difficult to construct a matching table, but the arguments described above can still be used with some modifications. Ultimately, we find that we can account for all logarithmic terms using the expansions

$$\xi(s) = s + n^{-1}(\log n)(s - \tfrac{1}{2})\tilde{p}^* + n^{-1}\left[\frac{\log(1-s) - \log(s)}{\pi^2} + (s - \tfrac{1}{2})\tilde{p}\right] + o(n^{-1})$$

and

$$\chi(i) = \chi_0(i) + n^{-1}(\log n)\tilde{\chi}^*(i) + n^{-1}\tilde{\chi}(i) + o(n^{-1}). \tag{83}$$

Matching between the bulk and the boundary layer can then be achieved by setting $\tilde{p}^* = \frac{2}{\pi^2}$, and taking

$$\tilde{p} = 2\lim_{i\to\infty}\left[i - \chi_0(i)\right].$$

While we have concentrated on obtaining terms up to ord$[n^{-(a-1)}]$ in our expansions of both ξ and χ, it may be noted that further high order terms can also be obtained using the techniques of matched asymptotic expansions. However, obtaining these high-order terms becomes much more algebraically laborious. In §A.1, we commented that finding higher-order corrections requires us to expand S_0 in (55) and exploiting the properties of $\chi(i)$. In the same way, obtaining higher order corrections in the boundary layer would require us to expand S_5 and S_6 in (70) and exploit the properties of $\xi(s)$. Additionally, we find that the high order solutions for ξ_k are no longer as simple as the expressions obtained when $b_k < a - 1$, which causes the matching table to become much more complicated.

As described in this section, formal asymptotic methods can be used to elucidate the structure of the original discrete problem and determine the appropriate scalings for higher-order asymptotic analsyis. By the principles of matched asymptotic expansions, we use information about the behaviour of the bulk solution to construct the boundary layer solution and vice versa; this is where formal asymptotic analysis becomes particularly useful. For example, our higher-order analysis of ξ gives us detailed information about the decay properties of χ_0. Indeed, combining (81), (82), and (83), we obtain the decay properties of χ_0 as given by (28), from which (4) follows.

In the general case where V satisfies (30), the coefficients of various terms change but the structure of the asymptotic matching remains identical up to ord$(n^{-(a-1)})$. Hence, we also find that the solution for $\tilde{\xi}$ given in (69) can be used to obtain information about the decay behaviour of χ_0 for a general V. From this, we find that we can generalise (4) to obtain (31).

B Technical details and computations of §4

Given the notation in §4, we prove inequalities (40a) and (40b) in Appendix B.1, and derive the second equality in (34) in Appendix B.2.

B.1 Proof of the inequalities (40a) and (40b) of Theorem 43

Proof (Proof of (40a)*)* Let $\varepsilon^n \xrightarrow{2} (\varepsilon, \hat{\varepsilon})$ such that $E_n^1(\varepsilon^n)$ is bounded. For the second term of $E_n^1(\varepsilon^n)$ in (34), we use the strong convergence of σ^n (see Lemma 42) to obtain

$$\left(\sigma^n, \varepsilon^n + \hat{\varepsilon}^n\right)_{\ell^2(\mathbb{N})} \xrightarrow{n\to\infty} \left(\sigma^\infty, \varepsilon + \hat{\varepsilon}\right)_{\ell^2(\mathbb{N})}. \tag{84}$$

We bound $Q_n(\varepsilon_n)$ in (34) from below by dropping some terms in the summation. We set $R_n := \lfloor n/2 \rfloor$, and estimate

$$Q_n(\varepsilon_n) = \sum_{k=1}^{n} \sum_{j=0}^{n-k} \phi_k\Big(\sum_{l=j+1}^{k+j} \varepsilon^n(l) \Big) \geq \sum_{k=1}^{R_n} \sum_{j=0}^{R_n-k} \Big[\phi_k\Big(\sum_{l=j+1}^{k+j} \varepsilon^n(l) \Big) + \phi_k\Big(\sum_{l=j+1}^{k+j} \hat{\varepsilon}^n(l) \Big) \Big].$$

To pass to the liminf as $n \to \infty$, we use Fatou's Lemma, by which we interpret the double sum as an integral over the lattice $\mathbb{N}_+^2$. We focus on the first term in the summand, because the second term involving $\hat{\varepsilon}^n$ can be estimated analogously. For the pointwise lower bound (as $n \to \infty$ with k and j fixed) of the summand, we interpret $\sum_{l=j+1}^{k+j} \varepsilon_l^n$ as an inner product of ε^n with an n-independent sequence consisting of 1's and 0's. Then the fact that $\varepsilon^{n,1/2} \rightharpoonup \varepsilon$ implies

$$\sum_{l=j+1}^{k+j} \varepsilon^{n,1/2}(l) \xrightarrow{n\to\infty} \sum_{l=j+1}^{k+j} \varepsilon(l) \qquad \text{for all } k, j \geq 1.$$

Since Lemma 41 implies that ϕ_k is positive and lower semicontinuous, it follows that

$$\liminf_{n\to\infty} \phi_k\Big(\sum_{l=j+1}^{k+j} \varepsilon_l^{n,1/2} \Big) \geq \phi_k\Big(\sum_{l=j+1}^{k+j} \varepsilon(l) \Big) \qquad \text{for all } k, j \geq 1.$$

This shows that the hypotheses of Fatou's Lemma are satisfied, and thus

$$\liminf_{n\to\infty} \sum_{k=1}^{n} \sum_{j=0}^{n-k} \phi_k\Big(\sum_{l=j+1}^{k+j} \varepsilon^n(l) \Big) \geq \sum_{k=1}^{\infty} \sum_{j=0}^{\infty} \Big[\phi_k\Big(\sum_{l=j+1}^{k+j} \varepsilon(l) \Big) + \phi_k\Big(\sum_{l=j+1}^{k+j} \hat{\varepsilon}(l) \Big) \Big].$$

Proof (Proof of (40b)*)* Let $(\varepsilon, \hat{\varepsilon}) \in \operatorname{Dom} E_\infty^1$ such that $E_\infty^1(\varepsilon, \hat{\varepsilon}) =: C < \infty$. Then $\varepsilon, \hat{\varepsilon} \in \ell^2(\mathbb{N}) \subset \ell^\infty(\mathbb{N})$, and

$$E_\infty^1(\varepsilon, \hat{\varepsilon}) \geq \phi_1\big(\varepsilon(i)\big) + \phi_1\big(\hat{\varepsilon}(j)\big) - \|\sigma^\infty\|_{\ell^2(\mathbb{N})} \|\varepsilon + \hat{\varepsilon}\|_{\ell^2(\mathbb{N})} \quad \text{for all } i, j \geq 1.$$

Hence, there exists a $\delta > 0$ such that

$$\varepsilon, \hat{\varepsilon} \in X_\delta := \Big\{ \varepsilon \in \ell^2(\mathbb{N}) \,\Big|\, \delta - 1 \leq \varepsilon(i) \leq \frac{1}{\delta}, \text{ for all } i \in \mathbb{N} \Big\}.$$

Next we construct a recovery sequence. As in [23], we note that the constraint that $\sum_{i=1}^{\infty} \varepsilon^n(i) = 0$ need not be preserved in the limit as $n \to \infty$. We take this into account by introducing $1 \ll S_n \ll n$ as the index where we match the boundary layer with the bulk. We note that as $n \to \infty$, it holds that $S_n \to \infty$ and $S_n/n \to 0$. We further set

$$u_n := \sum_{i=1}^{S_n} \varepsilon(i), \quad \text{and} \quad \hat{u}_n := \sum_{i=1}^{S_n} \hat{\varepsilon}(i). \tag{85}$$

We now define the recovery sequence

$$\varepsilon^n(i) := \begin{cases} \varepsilon(i) & i \in \{1, \dots, S_n\}, \\ -\dfrac{u_n + \hat{u}_n}{n - 2S_n} & i \in \{S_n + 1, \dots, n - S_n\}, \\ \hat{\varepsilon}(n + 1 - i) & i \in \{n - S_n + 1, \dots, n\}. \end{cases} \tag{86}$$

It is easily checked that $\sum_{i=1}^{n} \varepsilon^n(i) = 0$ and $\varepsilon^n(i) \geq -1$ for n large enough, hence $\varepsilon^n \in \operatorname{Dom} E_n^1$.

To show that $\varepsilon^n \xrightarrow{2} (\varepsilon, \hat{\varepsilon})$, we prove that $\varepsilon^{n,1/2} \to \varepsilon$ in $\ell^2(\mathbb{N})$, and conclude by an analogous argument that $\hat{\varepsilon}^{n,1/2} \to \hat{\varepsilon}$ in $\ell^2(\mathbb{N})$. To this end, we estimate

$$\|\varepsilon - \varepsilon^{n,1/2}\|_{\ell^2(\mathbb{N})}^2 = \sum_{i=S_n+1}^{\lceil n/2 \rceil} \big(\varepsilon(i) + \tfrac{u_n + \hat{u}_n}{n - 2S_n}\big)^2 + \sum_{i=\lceil n/2 \rceil + 1}^{\infty} \varepsilon(i)^2 \leq 2 \sum_{i=S_n+1}^{\lceil n/2 \rceil} \big(\tfrac{u_n + \hat{u}_n}{n - 2S_n}\big)^2 + 2 \sum_{i=S_n+1}^{\infty} \varepsilon(i)^2. \tag{87}$$

The second term in the right-hand side of (87) converges to 0 as $n \to \infty$ because $\varepsilon \in \ell^2(\mathbb{N})$. To show that the first term in the right-hand side is also small for large n, we interpret u_n in (85) as the inner product of ε with a sequence consisting of 1's and 0's. Applying the Cauchy-Schwartz inequality on this inner product yields

$$\sum_{i=S_n+1}^{\lceil n/2 \rceil} \left(\frac{u_n + \hat{u}_n}{n - 2S_n} \right)^2 \leq \frac{1}{(n - 2S_n)^2} \sum_{i=S_n+1}^{\lceil n/2 \rceil} \big(2\sqrt{S_n} \|\varepsilon\|_{\ell^2(\mathbb{N})}\big)^2 \lesssim \frac{1}{n^2} \frac{n}{2} 4S_n \|\varepsilon\|_{\ell^2(\mathbb{N})}^2 \xrightarrow{n\to\infty} 0,$$

where we recall that $S_n \ll n$ as $n \to \infty$. This completes the proof of $\varepsilon^n \xrightarrow{2} (\varepsilon, \hat{\varepsilon})$.

To establish the limsup inequality (40b), we observe from the argument leading to (84) that it is enough to focus on Q_n in (34), since the convergence of terms involving σ^n is implied by the fact that $\varepsilon^n \xrightarrow{2} (\varepsilon, \hat{\varepsilon})$, as just shown. For convenience, we choose S_n to be even. We split the summation in Q_n into four parts:

$$Q_n(\varepsilon^n) = \sum_{k=1}^{S_n/2}\left[\sum_{j=0}^{S_n-k}\phi_k\Big(\sum_{l=j+1}^{k+j}\varepsilon^n(l)\Big) + \sum_{j=S_n-k+1}^{n-S_n-1}\phi_k\Big(\sum_{l=j+1}^{k+j}\varepsilon^n(l)\Big) + \sum_{j=n-S_n}^{n-k}\phi_k\Big(\sum_{l=j+1}^{k+j}\varepsilon^n(l)\Big)\right] + \sum_{k=1+S_n/2}^{n}\sum_{j=0}^{n-k}\phi_k\Big(\sum_{l=j+1}^{k+j}\varepsilon^n(l)\Big). \quad (88)$$

The first and third term are constructed to contain only those elements of $\varepsilon^n(l)$ which equal either $\varepsilon(l)$ or $\hat{\varepsilon}(l)$. Using this observation, we estimate these terms by

$$\sum_{k=1}^{S_n/2}\left[\sum_{j=0}^{S_n-k}\phi_k\Big(\sum_{l=j+1}^{k+j}\varepsilon^n(l)\Big) + \sum_{j=n-S_n}^{n-k}\phi_k\Big(\sum_{l=j+1}^{k+j}\varepsilon^n(l)\Big)\right] \le \sum_{k=1}^{\infty}\sum_{j=0}^{\infty}\left[\phi_k\Big(\sum_{l=j+1}^{k+j}\varepsilon(l)\Big) + \phi_k\Big(\sum_{l=j+1}^{k+j}\hat{\varepsilon}(l)\Big)\right].$$

Since the right-hand side equals the first two terms of E^1_∞ given by Q_∞ and $\hat{Q}_\infty$, it remains to show that the second and fourth term in (88) converge to 0 as $n \to \infty$.

We start by proving that the second term is small for large n. We observe that it solely contains those elements of $\varepsilon^n(i)$ which equal either entries of the tails of ε and $\hat{\varepsilon}$, or equal the (small) constant term in (86). For this reason, it turns out to be enough to bound the second term by employing the quadratic upper bound of ϕ_k given by Lemma 41 (it applies because of $\varepsilon^n \in X_\delta$), and then applying Jensen's inequality. In more detail

$$\begin{aligned}\sum_{k=1}^{S_n/2}\sum_{j=S_n-k+1}^{n-S_n-1}\phi_k\Big(\sum_{l=j+1}^{k+j}\varepsilon^n(l)\Big) &\le \sum_{k=1}^{S_n/2}\sum_{j=S_n-k+1}^{n-S_n-1}\frac{C_\delta}{k^{a+2}}k^2\Big(\frac{1}{k}\sum_{l=j+1}^{k+j}\varepsilon^n(l)\Big)^2 \\ &\le \sum_{k=1}^{S_n/2}\frac{C_\delta}{k^{a+1}}\sum_{j=S_n-k+1}^{n-S_n-1}\sum_{l=j+1}^{k+j}\big|\varepsilon^n(l)\big|^2 \le \sum_{k=1}^{S_n/2}\frac{C_\delta}{k^{a+1}}\sum_{i=S_n/2+2}^{n-S_n/2-1}k\big|\varepsilon^n(i)\big|^2 \\ &\le \Big(\sum_{k=1}^{\infty}\frac{C_\delta}{k^a}\Big)\left[\sum_{i=S_n/2}^{\infty}\big(|\varepsilon(i)|^2+|\hat{\varepsilon}(i)|^2\big) + \sum_{i=S_n+1}^{n-S_n}\Big(\frac{u_n+\hat{u}_n}{n-2S_n}\Big)^2|\varepsilon^n(i)|^2\right],\end{aligned}$$

in which the right-hand side converges to 0 as $n \to \infty$ by the same argument that we use for showing the convergence of the right-hand side in (87).

Finally, we show that the fourth term in (88) converges to 0. Since k (the distance between particles in terms of their index) is large, we use similar arguments in the following estimate

$$\begin{aligned}\sum_{k=1+S_n/2}^{n}\sum_{j=0}^{n-k}\phi_k\Big(\sum_{l=j+1}^{k+j}\varepsilon^n(l)\Big) &\le \sum_{k=1+S_n/2}^{n}\sum_{j=0}^{n-k}\frac{C_\delta}{k^{a+2}}k^2\Big(\frac{1}{k}\sum_{l=j+1}^{k+j}\varepsilon^n(l)\Big)^2 \\ &\le \sum_{k=1+S_n/2}^{n}\frac{C_\delta}{k^{a+1}}\sum_{j=0}^{n-k}\sum_{l=j+1}^{k+j}\big|\varepsilon_l^n\big|^2 \le \sum_{k=1+S_n/2}^{n}\frac{C_\delta}{k^a}\sum_{i=1}^{n}\big|\varepsilon^n(i)\big|^2 = C_\delta\|\varepsilon^n\|^2_{\ell^2(\mathbb{N})}\sum_{k=1+S_n/2}^{n}\frac{1}{k^a},\end{aligned}$$

which converges to 0 as $n \to \infty$ since $a > 3/2 > 1$.

B.2 Computation of σ^n

In this section we fix n, and show that

$$\sum_{k=1}^{n}\sum_{j=0}^{n-k}\sum_{l=j+1}^{k+j}V'(k)\varepsilon(l) = \sigma\cdot(\varepsilon+\hat{\varepsilon}), \quad (89)$$

where σ is given by (35), i.e.

$$\sigma_i = \sum_{k=i+1}^{n-i} \big[(k-i)\wedge(n-i+1-k)\big]\big|V'(k)\big| \quad \text{for } i=\{1,\dots,\lfloor n/2\rfloor\}.$$

We start by changing the order of summation in

$$\sum_{k=1}^{n} V'(k)\sum_{j=0}^{n-k}\sum_{l=j+1}^{k+j}\varepsilon(l) = \sum_{k=1}^{n}\sum_{l=1}^{n}\varepsilon(l)V'(k)\sum_{j=0\vee(l-k)}^{(n-k)\wedge(l-1)} 1$$
$$= \sum_{k=1}^{n}\sum_{l=1}^{n} V'(k)\big[k\wedge l\wedge(n-k+1)\wedge(n-l+1)\big]\varepsilon(l) =: v\cdot\tilde{A}\varepsilon,$$

where the vector $v\in\mathbb{R}^n$ is defined by $v_k := V'(k) < 0$, and the matrix $\tilde{A}\in\mathbb{R}^{n\times n}$ is illustrated in Figure 13.

Since $\varepsilon\cdot\mathbf{1}=0$, it holds that $\tilde{A}\varepsilon = (\tilde{A}-B)\varepsilon$ for any matrix B whose rows are multiples of $\mathbf{1}$. We take B such that the entries in its i-th row equal $i\wedge(n-i+1)$, and set $A := -(\tilde{A}-B)^T$ (see Figure 13 for its structure). Then

$$v\cdot\tilde{A}\varepsilon = -v\cdot A^T\varepsilon = -\varepsilon\cdot Av = \sum_{l=1}^{\lfloor n/2\rfloor}\big[(-Av)(l)\varepsilon(l) + (-Av)(n-l+1)\hat{\varepsilon}(l)\big].$$

From Figure 13 it is easy to see that the vector $-Av$ has reversal symmetry, and (89) follows.

Acknowledgements The authors would like to thank Mark Peletier for valuable discussions, and TU Eindhoven for providing funds to cover research visits by TH and CH. TH and PvM would also like to thank the Hausdorff Research Institute for Mathematics in Bonn for hosting them during the junior workshop 'Analytic approaches to scaling limits for random systems' during which work on this project was carried out.

Conflict of interest: The authors declare that there is no conflict of interest regarding this work.

References

1. Bernoff, A.J., Topaz, C.M.: Nonlocal aggregation models: a primer of swarm equilibria [reprint of mr2788924]. SIAM Rev. **55**(4), 709–747 (2013). DOI 10.1137/130925669
2. Bethuel, F., Brezis, H., Hélein, F.: Ginzburg-Landau Vortices, vol. 13. Springer Science & Business Media (2012)
3. Blanc, X., Le Bris, C., Lions, P.L.: Atomistic to continuum limits for computational materials science. M2AN Math. Model. Numer. Anal. **41**(2), 391–426 (2007). DOI 10.1051/m2an:2007018

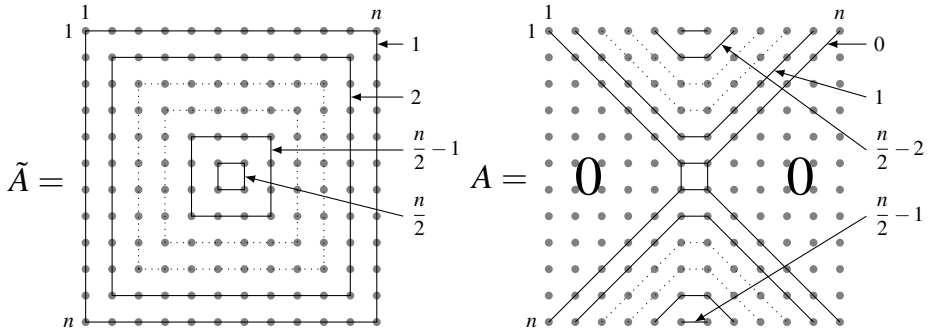

Fig. 13 Schematic picture of the two index matrices $\tilde{A}$ and $A=\tilde{A}-B$. The lines are level sets which connect entries with the same value. We have taken n to be even for convenience.

4. Braides, A.: Γ-convergence for beginners, *Oxford Lecture Series in Mathematics and its Applications*, vol. 22. Oxford University Press, Oxford (2002). DOI 10.1093/acprof:oso/9780198507840.001.0001
5. Braides, A., Cicalese, M.: Surface energies in nonconvex discrete systems. Math. Models Methods Appl. Sci. **17**(7), 985–1037 (2007). DOI 10.1142/S0218202507002182
6. Braides, A., Dal Maso, G., Garroni, A.: Variational formulation of softening phenomena in fracture mechanics: the one-dimensional case. Arch. Ration. Mech. Anal. **146**(1), 23–58 (1999). DOI 10.1007/s002050050135
7. Braides, A., Truskinovsky, L.: Asymptotic expansions by Γ-convergence. Continuum Mechanics and Thermodynamics **20(1)**, 21–62 (2008)
8. Brauchart, J.S., Hardin, D.P., Saff, E.B.: The next-order term for optimal Riesz and logarithmic energy asymptotics on the sphere. Contemporary Mathematics **578**, 31–61 (2012)
9. Carrier, G.F., Krook, M., Pearson, C.E.: Functions of a Complex Variable – Theory and Technique. SIAM (2005)
10. Castellano, C., Fortunato, S., Loreto, V.: Statistical physics of social dynamics. Rev. Mod. Phys. **81**, 591–646 (2009). DOI 10.1103/RevModPhys.81.591
11. Comtet, L.: Advanced Combinatorics: The art of finite and infinite expansions. D. Reidel Publishing COmpany (1974)
12. Dal Maso, G.: An introduction to Γ-convergence. Progress in Nonlinear Differential Equations and their Applications, 8. Birkhäuser Boston, Inc., Boston, MA (1993). DOI 10.1007/978-1-4612-0327-8
13. Dyson, F.J.: Statistical theory of the energy levels of complex systems. i. Journal of Mathematical Physics **3**(1), 140–156 (1962)
14. Flatley, L.C., Theil, F.: Face-centered cubic crystallization of atomistic configurations. Arch. Ration. Mech. Anal. **218**(1), 363–416 (2015). DOI 10.1007/s00205-015-0862-1
15. Garroni, A., van Meurs, P., Peletier, M.A., Scardia, L.: Boundary-layer analysis of a pile-up of walls of edge dislocations at a lock. Mathematical Models and Methods in Applied Sciences **26**(14), 2735–2768 (2016)
16. Geers, M.G.D., Peerlings, R.H.J., Peletier, M.A., Scardia, L.: Asymptotic behaviour of a pile-up of infinite walls of edge dislocations. Archive for Rational Mechanics and Analysis **209**, 495–539 (2013)
17. Gladwell, G.M.: Contact problems in the classical theory of elasticity. Springer Science & Business Media (1980)
18. Hall, C.L.: Asymptotic expressions for the nearest and furthest dislocations in a pile-up against a grain boundary. Philosophical Magazine **90**(29), 3879–3890 (2010)
19. Hall, C.L.: Asymptotic analysis of a pile-up of regular edge dislocation walls. Materials Sceince and Engineering A **530**, 144–148 (2011)
20. Hall, C.L., Chapman, S.J., Ockendon, J.R.: Asymptotic analysis of a system of algebraic equations arising in dislocation theory. SIAM Journal on Applied Mathematics **70**(7), 2729–2749 (2010)
21. Hinch, E.J.: Perturbation Methods. Cambridge University Press (1991)
22. Hirth, J.P., Lothe, J.: Theory of Dislocations, 2nd edn. John Wiley & Sons (1982)
23. Hudson, T.: Gamma-expansion for a 1D confined Lennard-Jones model with point defect. Netw. Heterog. Media **8**(2), 501–527 (2013). DOI 10.3934/nhm.2013.8.501
24. Ivanov, V.A., Rodionova, A.S., Martemyanova, J.A., Stukan, M.R., Müller, M., Paul, W., Binder, K.: Wall-induced orientational order in athermal semidilute solutions of semiflexible polymers: Monte Carlo simulations of a lattice model. J Chem Phys **138**, 234,903 (2013). DOI 10.1063/1.4810745
25. Jones, J.E.: On the determination of molecular fields. ii. from the equation of state of a gas. Proceedings of the Royal Society of London A: Mathematical, Physical and Engineering Sciences **106**(738), 463–477 (1924). DOI 10.1098/rspa.1924.0082
26. Landkof, N.S.: Foundations of Modern Potential Theory, vol. 180. Springer (1972)
27. Lee, A.A., Kondrat, S., Kornyshev, A.A.: Single-file charge storage in conducting nanopores. Physical Review Letters **113**(4), 048,701 (2014). DOI http://dx.doi.org/10.1103/PhysRevLett.113.048701
28. Lyness, J.N.: Approximation and Computation: A Festschrift in Honor of Walter Gautschi, vol. 119, chap. Finite-part integrals and the Euler–Maclaurin expansion, pp. 297–407. Birkhäuser Boston (1993)
29. Metropolis, N., Rosenbluth, A.W., Rosenbluth, M.N., Teller, A.H., Teller, E.: Equation of state calculations by fast computing machines. The Journal of Chemical Physics **21**(6), 1087–1092 (1953)
30. van Meurs, P., Muntean, A.: Upscaling of the dynamics of dislocation walls. Adv. Math. Sci. Appl. **24**(2), 401–414 (2014)
31. van Meurs, P., Muntean, A., Peletier, M.A.: Upscaling of dislocation walls in finite domains. European Journal of Applied Mathematics **25(6)**, 749–781 (2014). DOI 10.1017/S0956792514000254
32. Monegato, G., Lyness, J.N.: The euler–maclaurin expansion and finite-part integrals. Numerische Mathematik **81**, 273–291 (1998)
33. Nussinov, Z., van den Brink, J.: Compass models: Theory and physical motivations. Reviews of Modern Physics **87**, 1–59 (2015). DOI 10.1103/RevModPhys.87.1

34. Petrache, M., Serfaty, S.: Next order asymptotics and renormalized energy for riesz interactions. Journal of the Institute of Mathematics of Jussieu pp. 1–69 (2014)
35. Russo, G., Smereka, P.: Computation of strained epitaxial growth in three dimensions by kinetic monte carlo. Journal of Computational Physics **214**(2), 809–828 (2006)
36. Saff, E.B., Kuijlaars, A.B.: Distributing many points on a sphere. The Mathematical Intelligencer **19**(1), 5–11 (1997)
37. Scardia, L., Schlömerkemper, A., Zanini, C.: Boundary layer energies for nonconvex discrete systems. Math. Models Methods Appl. Sci. **21**(4), 777–817 (2011). DOI 10.1142/S0218202511005210
38. Schaarwächter, W., Ebener, H.: Acoustic emission: A probe into dislocation dynamics in plasticity. Acta Metallurgica et Materialia **38**(2), 195 – 205 (1990). DOI http://dx.doi.org/10.1016/0956-7151(90)90049-M
39. Sidi, A.: Euler–Maclaurin expansions for integrals with arbitrary algebraic-logarithmic endpoint singularities. Constructive Approximation **36**, 331–352 (2012)
40. Szlufarska, I.: Atomistic simulations of nanoindentation. Materials Today **9**(5), 42 – 50 (2006). DOI http://dx.doi.org/10.1016/S1369-7021(06)71496-1
41. Theil, F.: A proof of crystallization in two dimensions. Comm. Math. Phys. **262**(1), 209–236 (2006). DOI 10.1007/s00220-005-1458-7
42. Thomas, J.M., Thomas, W.J.: Principles and practice of heterogeneous catalysis. John Wiley & Sons (2014)
43. Voskoboinikov, R.E., Chapman, S.J., Mcleod, J.B., Ockendon, J.R.: Asymptotics of edge dislocation pile-up against a bimetallic interface. Mathematics and Mechanics of Solids **14**(1-2), 284 – 295 (2009). DOI 10.1177/1081286508092616
44. Wales, D.J., Doye, J.P.K.: Global optimization by basin-hopping and the lowest energy structures of lennard-jones clusters containing up to 110 atoms. The Journal of Physical Chemistry A **101**(28), 5111–5116 (1997). DOI 10.1021/jp970984n
45. Wang, W., Wang, T.: General identities on Bell polynomials. Computers and Mathematics with Applications (2009)
46. Wennberg, C.L., Murtola, T., Hess, B., Lindahl, E.: Lennard–Jones lattice summation in bilayer simulations has critical effects on surface tension and lipid properties. J Chem Theory Comput **9**(8), 3527–3537 (2013). DOI 10.1021/ct400140n
47. Wigner, E.P.: Characteristic vectors of bordered matrices with infinite dimensions. Annals of Mathematics pp. 548–564 (1955)
48. Zschocke, F., Vojta, M.: Physical states and finite-size effects in Kitaev's honeycomb model: Bond disorder, spin excitations, and NMR line shape. Phys. Rev. B **92**, 014,403 (2015). DOI 10.1103/PhysRevB.92.014403